DOI: 10.1590/2317-4889201720160086

ARTICLE

Petrogenesis and age of skarns associated with felsic and metamafic dykes from the Paraíba do Sul Complex, southern Espírito Santo State

Petrogênese e idade de escarnitos associados a diques félsicos e metamáficos do Complexo Paraíba do Sul, sul do Espírito Santo

Raissa Beloti de Mesquita[1]*, Hanna Jordt-Evangelista[2], Gláucia Nascimento Queiroga[2], Edgar Batista de Medeiros Júnior[2], Ivo Antônio Dussin[3]

ABSTRACT: This paper concerns the study of petrography, mineral chemistry and geochronology of skarns generated at the contact of marbles of the Paraíba do Sul Complex with felsic and metamafic dykes in the southern Espírito Santo State. The marbles were metamorphosed under P-T granulite facies conditions during the syn-collisional stage of the Neoproterozoic Araçuaí orogen. Metamafic bodies are composed of amphibolite and hornblende granofels, while felsic dykes consist of alkali-feldspar granite, monzogranite or syenogranite. From marble towards the dyke, skarns related to the metamafic bodies are composed of *carbonate + olivine* and *diopside + hornblende* zones. Skarn associated to the granitic dykes are composed of three different zones: *carbonate + tremolite*, *diopside*, *scapolite + diopside*. Variations in mineral chemical compositions along the metasomatic zones suggest introduction of Mg and Ca from the marbles, Fe from the metamafic dykes and Na from the granitoids. The presence of spinel in the metamafic dykes and their skarns indicates that both were metamorphosed under granulite facies conditions during the 580–560 Ma syn-collisional stage. U-Pb zircon geochronology (LA-ICP-MS) of an alkali-feldspar granite dyke resulted in a crystallization age of *ca.*540 Ma, which suggests that its skarns are therefore younger than skarns associated with the syn-collisional metamafic dykes.

KEYWORDS: skarns; petrogenesis; geochronology; Paraíba do Sul Complex.

RESUMO: *Este trabalho apresenta o estudo de petrografia, química mineral e geocronologia de escarnitos gerados no contato de mármores do Complexo Paraíba do Sul com diques metamáficos e félsicos, no sul do Espírito Santo. Os mármores foram metamorfizados sob condições de pressão e temperatura da fácies granulito durante a fase sin-colisional do orógeno neoproterozoico Araçuaí. Os corpos metamáficos são compostos de anfibolito e hornblenda granofels, enquanto os diques félsicos consistem de álcali-feldspato granito, monzogranito ou sienogranito. Do mármore para o dique, escarnitos associados com os diques metamáficos são compostos das zonas carbonato + olivina e diopsídio + hornblenda. Escarnitos associados com os diques graníticos são compostos de três zonas mineralógicas distintas: carbonato + tremolita, diopsídio e escapolita + diopsídio. Variações na composição química mineral ao longo das zonas metassomáticas sugerem introdução de Mg e Ca dos mármores, Fe dos diques metamáficos e Na dos granitos. A presença de espinélio nos diques metamáficos e em seus escarnitos indica que ambos foram metamorfizados sob condições de fácies granulito durante o estágio sin-colisional (580–560 Ma). A geocronologia U-Pb via LA-ICP-MS em zircões de um dique de álcali-feldspatogranito resultou em uma idade de cristalização de ca.540 Ma, o que sugere que seus escarnitos são, portanto, mais novos que os escarnitos associados com os diques metamáficos sin-colisionais.*

PALAVRAS-CHAVE: *escarnitos; petrogênese; geocronologia; Complexo Paraíba do Sul.*

[1]Serviço Geológico do Brasil – CPRM; Programa de Pós-graduação em Evolução Crustal e Recursos Naturais, Departamento de Geologia, Escola de Minas, Universidade Federal de Ouro Preto – UFOP, Ouro Preto (MG), Brazil. *E-mail: raissa.mesquita@cprm.gov.br*

[2]Departamento de Geologia, Escola de Minas, Universidade Federal de Ouro Preto – UFOP, Ouro Preto (MG), Brazil. *E-mails: hanna@degeo.ufop.br; glauciaqueiroga@yahoo.com.br; edgarjr@ymail.com*

[3]Programa de Pós-Graduação em Geologia, Instituto de Geociências/Centro de Pesquisa Manoel Teixeira da Costa (IGC-CPMTC), Universidade Federal de Minas Gerais – UFMG, Belo Horizonte (MG), Brazil; Programa de Pós-Graduação em Análise de Bacias e Faixas Móveis, Faculdade de Geologia, Universidade Estadual do Rio de Janeiro – UERJ, Rio de Janeiro (RJ), Brazil. *E-mail: ivodusin@yahoo.com.br*

*Corresponding author.

Manuscript ID: 20160086. **Received in:** 07/17/2016. **Approved in:** 05/05/2017.

INTRODUCTION

The southern region of the Espírito Santo State in Brazil stands out for the exploitation of dimension stones, mainly of marble. The marble quarries are distributed in a lens-shaped body that outcrops between Cachoeiro de Itapemirim and Vargem Alta municipalities, occurring also in smaller bodies in Castelo (Fig. 1). Metamafic dykes of amphibolite and felsic dykes of granite are intruded in these occurrences of marble. In general, the felsic dykes do not show evidence of deformation and metamorphism. The mafic dykes, in contrast, were intensely deformed, metamorphosed and transformed into amphibolite. Skarns were formed at the contacts between the dykes and the marble, and show zones with distinct mineralogical compositions due to migration of chemical components because of the chemical contrast caused by the distinct compositions of the lithotypes.

The purpose of this work was to provide information on the age and on the metamorphic/metasomatic processes that led to skarn formation using detailed petrography, mineral chemistry and geochronology.

GEOLOGICAL SETTING

The study region belongs to the crystalline core of the Araçuaí orogen composed of rocks related to the Paraíba do Sul Complex, besides pre-collisional and post-collisional intrusive rocks (Fig. 1). The Araçuaí orogen encompasses the Araçuaí fold belt and the high-grade crystalline core. To the west, it is limited by the São Francisco Craton (Almeida 1977), and to the east by the Atlantic coast. This orogen and the West Congo Belt that is situated on the western border of the African Congo Craton make up the Brasiliano/Pan-African system of orogens of the West Gondwana (Porada, 1989; Pedrosa-Soares *et al.*1992) referred in the literature as the Araçuaí-West Congo orogen.

The Paraíba do Sul Complex was subdivided by Vieira (1997) into nine units that comprise a metasedimentary sequence at the base and a metavolcano-sedimentary sequence on the top. The units embrace gneisses with intercalations of calc-silicate rocks, quartzites, amphibolites and the marbles studied in this work. The sediments of the Paraíba do Sul Complex were deposited in a back-arc basin with a maximum depositional age of 619 Ma (Medeiros Junior 2016).

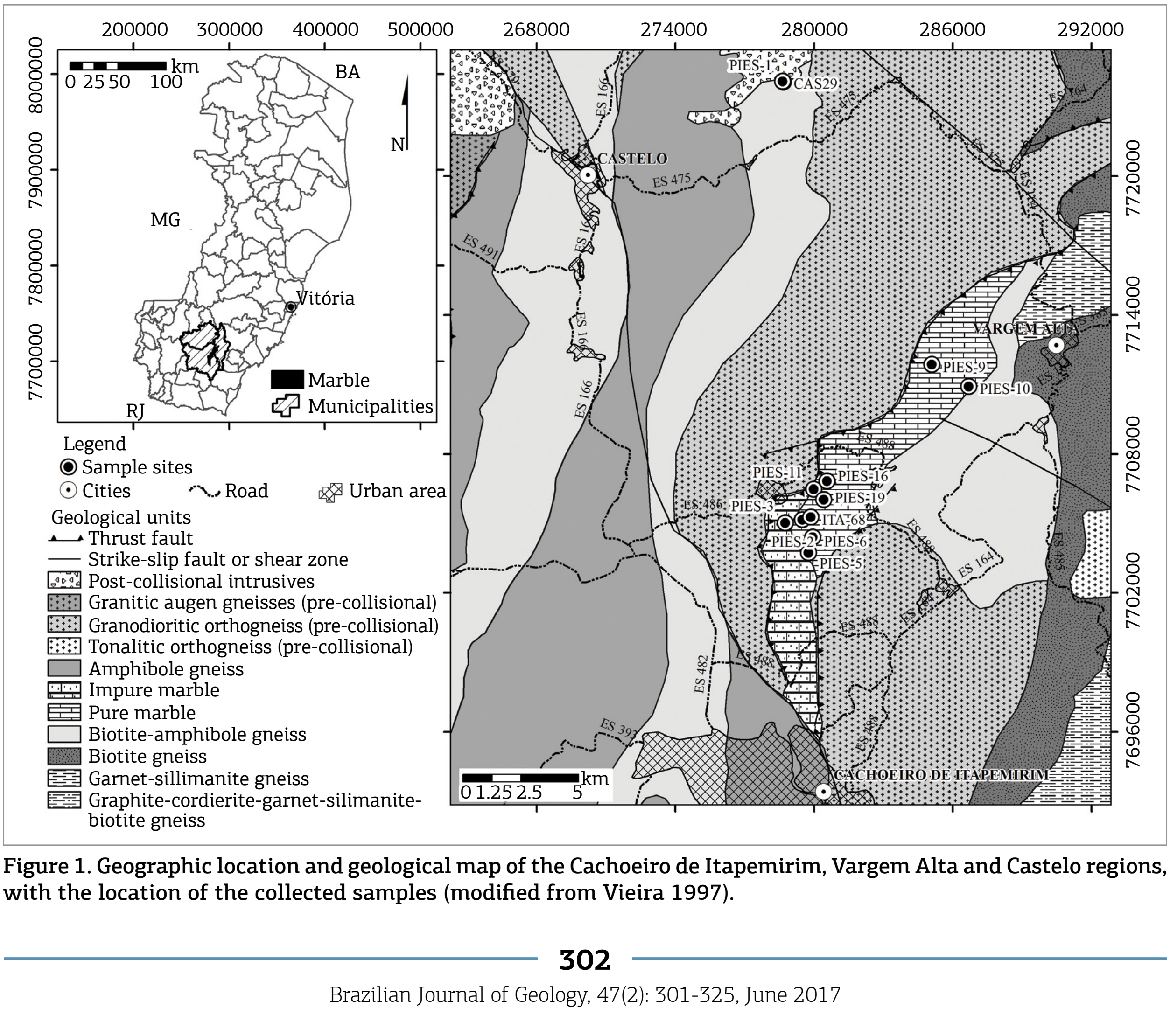

Figure 1. Geographic location and geological map of the Cachoeiro de Itapemirim, Vargem Alta and Castelo regions, with the location of the collected samples (modified from Vieira 1997).

The Paraíba do Sul rocks can be correlated to the Nova Venécia Complex, located in the northern region of the Espírito Santo State, which has a maximum depositional age of *ca.*631 Ma (Noce *et al.* 2004). The metamorphic event that affected this set of rocks is correlated to the syn-collisional stage of the edification of the Araçuaí orogen between 580 and 560 Ma (Pedrosa-Soares *et al.* 2001, 2007). Medeiros Junior (2016) determined temperatures between 750 and 800ºC for this metamorphic event. This complex, according to Tupinambá *et al.* (2007), can be correlated to the high-grade metasedimentary rocks and orthogneisses of the Costeiro Domain of the northern sector of the Ribeira Belt.

The pre-collisional gneissic rocks correspond to the G1 Supersuite of Pedrosa-Soares *et al.* (2007, 2011) formed between ca. 630 and 580 Ma. They comprehend amphibolite facies, calc-alkaline granitic to tonalitic orthogneisses.

The post-collisional intrusive rocks are associated with the G5 Supersuite, generated between 520 and 490 Ma (Söllner *et al* .1991, Noce *et al.* 1999 *apud* Pedrosa-Soares & Wiedemann-Leonardos 2000). The G5 Supersuite is represented mainly by rocks of granitic composition with subordinated mafic rocks (Vieira 1997).

The main occurrence of marble in the Cachoeiro de Itapemirim region consists of a lens-shaped body that extends for at least 25 km in northeast–southwest direction with a width of about 4 km. Another occurrence is located northwest of the main lens, in the region of Castelo. Paragneisses of the Paraíba do Sul Complex and pre-collisional granodioritic orthogneisses also occur in the study area. Outstanding expositions can be observed in the marble quarries.

The marble is in general very pure, being composed mainly of dolomite and of rare calcitic layers and lenses. Locally, it shows metamorphic bands rich in calc-silicate minerals that present a N-S foliation dipping to the E, besides west-vergent folds and boudins (Jordt-Evangelista & Viana 2000).

The mineralogy of the marble, its silicate portions, the granitic and metamafic dykes, as well as the skarnitic zones, were described by Jordt-Evangelista and Viana (2000) and Oliveira (2012) in the Cachoeiro de Itapemirim region. Due to the rare presence of spinel, the marble and the skarns generated at the contact with the metamafic dykes were formed under granulite facies conditions and were partially affected by retrometamorphic transformations (Jordt-Evangelista & Viana 2000). The metamorphic temperatures of the marbles and calc-silicate rocks of the Paraíba do Sul Complex in the study region range between 690 to 790ºC (Medeiros Junior 2016).

MATERIALS AND METHODS

Representative samples of the different lithotypes were collected from 10 outcrops (Fig. 1), of which 47 thin sections were made. In addition, 10 thin sections from Medeiros Junior (2016) (ITA-68 and CAS29) and 10 thin sections from Oliveira (2012) (ESC) were incorporated in this work.

The thin sections were examined under transmitted and reflected light microscopy at the Departamento de Geologia (DEGEO) of the Universidade Federal de Ouro Preto (UFOP) and at the Laboratório de Análises Minerais (LAMIN) of Superintendência Regional de Manaus do Serviço Geológico do Brasil (CPRM). Quantitative and semi-quantitative analyses of mineral chemistry were obtained using the electron microprobe (EMP) Jeol Superprobe JXA-8900RL, at 15 kV, and a beam current of 20 nA, at the Centro de Microscopia of the Universidade Federal de Minas Gerais (UFMG), and the scanning electronic microscope (SEM) Jeol JSM-6010LA with a coupled energy dispersive spectrometer (EDS), at 20 kV, and spot size of 70, at the Laboratório de Microanálises of DEGEO/UFOP. The mineral chemistry data were processed with Minpet® software version 2.02 (Richard 1995).

U-Pb geochronology by LA-ICP-MS (Laser Ablation Inductively Coupled Plasma Mass Spectrometer) analyses were performed on zircon grains from an alkali-feldspar granitic dyke sample. The dated granite was selected because of the lack of any metamorphic overprinting, so that skarns were essentially generated by the post-tectonic intrusion. The zircon concentrate was prepared at the Laboratório de Preparação de Amostras para Geoquímica e Geocronologia (LOPAG) of DEGEO/UFOP using conventional jaw crusher, milling, manual panning, heavy liquids separation and magnetic-Frantz isodynamic separator. Subsequently, the zircons were handpicked under binocular microscope and mounted on an epoxy disk. The mount was polished and imaged under cathodoluminescence, using a scanning electronic microscope Quanta-250-FEI with cathodoluminescence detector of Oxford Instruments Co. at the Laboratório Multiusuário de Meio Ambiente e Materiais (MULTILAB) of the Universidade do Estado do Rio de Janeiro. The laser ablation-ICP-MS (LA-ICP-MS) analyses were performed using an Agilent 7700 Q-ICP-MS and a 213 nm New Wave laser at the Laboratório de Geoquímica Isotópica of DEGEO/UFOP (see Romano *et al.* 2013 and Takenaka *et al.*2015 for details on the instrumentation and methodology). The standard M127 zircon (Nasdala *et al.* 2008) was used during the runs. The relevant isotopic ratios were calculated using the data reduction software Glitter (van Achterbergh *et al.* 2001), and the U-Pb diagrams were produced using the software Isoplot 3.75 (Ludwig 2012).

FIELD AND PETROGRAPHIC ASPECTS

Metamafic dykes

The metamafic rocks occur as 7 cm to 1.5 m wide dykes and lens-shaped bodies that are stretched parallel to the marble foliation. The dykes are intensely deformed, boudinated, folded, disrupted and metamorphosed (Fig. 2A). The intense deformation does not allow to exclude the possibility that the mafic bodies could have originally been flows coeval with the carbonate rocks. They are composed of amphibolite and hornblende granofels. The amphibolite is dark gray to black, fine-grained, and the mafic minerals are oriented parallel to the regional foliation. The hornblende granofels is black, fine-grained and does not show foliation. Usually, there are phlogopite-rich films along the borders of the dykes; in some cases, the dyke seems to be completely transformed into this mineral. Garnet and clinopyroxene porphyroblasts occur in the largest dykes.

The amphibolite consists essentially of pargasite (50 to 60 vol%) and plagioclase (30 to 40%) (Fig. 2B), with minor amounts of biotite (3 to 15%) and opaque minerals (2 to 5%). Titanite, apatite, zircon and rare clinopyroxene occur as accessories. Sericite, epidote, carbonate, chlorite and calcic scapolite (see mineral chemistry) occur as secondary minerals. Pargasite (see mineral chemistry) is subidioblastic to idioblastic and presents greenish to brownish pleochroism. Plagioclase occurs as xenoblastic and sometimes porphyroblastic grains that display interlobate to polygonal contacts and intense sericitization, saussuritization and scapolitization (Fig. 2B). Often, it presents usually well-defined concentric extinction, due to compositional zoning. Brownish to reddish biotite can be poikiloblastic with inclusions of plagioclase, scapolite, opaque minerals and amphibole. The main opaque mineral is pyrrhotite, but subordinately chalcopyrite is also present.

The hornblende granofels is granoblastic, composed of pargasitic to tschermakitic hornblende (99 to 100 vol%), and scarce phlogopite, pyrrhotite and spinel. The amphibole is weakly pleochroic in shades of brown and yellow-brown. Rarely, green spinel is found associated with phlogopite.

Felsic dykes

The felsic dykes and sills are 10 cm to 2 m wide. Generally, they do not show any evidence of deformation (Fig. 2C and D), but dykes showing some metamorphic foliation were rarely observed.

The felsic dykes consist of alkali-feldspar granite, monzogranite and syenogranite. The syenogranite presents some metamorphic overprinting, but still preserves relicts of the igneous texture.

The largest of the studied skarns, 1.5 m wide, was found at the contact of an alkali-feldspar granite, which was chosen for geochronology. This granite is composed of alkali-feldspar (75 vol%), quartz (20%), plagioclase (2%), clinopyroxene (2% –hedenbergite, see mineral chemistry) and titanite, biotite, opaque minerals, allanite, apatite and zircon as accessory phases (1%). Typically, igneous tabular feldspars are observed (Fig. 2E). They may display a poikilitic texture with apatite and pyroxene inclusions. Quartz with undulatory extinction is an evidence of incipient deformation. Alkali-feldspar is perthitic and presents Tartan and Carlsbad twinning. Usually this feldspar is partially replaced by sericite and carbonate. Subhedral tabular plagioclase grains have a concentric extinction due to compositional zoning. Light green hedenbergite presents partial substitution by amphiboles.

The monzogranite presents anhedral granular and inequigranular seriate texture, with tabular plagioclase. It is composed of quartz (25 to 40 vol%), plagioclase (15 to 25%), alkali-feldspar (15 to 35%) and less than 1% of amphibole, clinopyroxene, biotite, sericite, titanite, apatite, garnet, zircon, monazite, epidote, Fe-Mg chlorite and opaque minerals. Quartz may show undulatory extinction. Plagioclase presents concentric extinction due to chemical zoning. It may be partially replaced by sericite, epidote and carbonate. Alkali-feldspar is commonly perthitic, has Tartan twinning and incipient sericitization. Amphibole is strongly pleochroic from olive-green to brownish-green, which is characteristic of hornblende. It may be partially replaced by biotite and carbonate. Fe-Mg chlorite may occur as alteration of biotite.

The syenogranite is distinguished from the other granitoids by the preferential orientation of biotite and hornblende. It is composed of quartz (25 to 30 vol%), alkali-feldspar (35 to 50%), plagioclase (5 to 15%), biotite (up to 5%), hornblende (up to 3%), clinopyroxene (up to 2%), and traces of titanite, garnet and zircon. Sericite, chlorite, epidote and carbonate may occur as secondary minerals. Quartz is granular and may be stretched parallel to the mafic mineral orientation. Undulatory extinction and dynamic recrystallization by subgrain rotation and by boundary migration occur as an evidence of deformation. Perthitic alkali-feldspar is often tabular-shaped. It presents Tartan and Carlsbad twinning and, frequently, alteration to sericite. Plagioclase is anhedral to subhedral, sometimes tabular-shaped, and may present concentric extinction. Alteration to sericite and epidote usually occurs. Clinopyroxene is weakly pleochroic in shades of light green to colorless and may occur partially replaced by hornblende. Hornblende is pleochroic from olive green to brownish-green. Biotite is dark brown, may replace hornblende and be replaced by chlorite.

Prg: pargasite; Pl: plagioclase; Phl: phlogopite; Scp: scapolite; Afs: alkali-feldspar; Hd: hedenbergite; Amp: amphibole; XPL: crossed polarized light; PPL: plane polarized light.

Figure 2. Photographs and photomicrographs of dykes: (A) deformed mafic dykes (PIES-6); (B) photomicrograph of amphibolite (PIES-2F2); (C) granitic dyke (PIES-10); (D) outcrop of alkali-feldspar granite; (E) photomicrograph of alkali-feldspar granite with tabular alkali-feldspar (XPL); (F) photomicrograph of alkal--feldspar granite with hedenbergite with marginal substitution by amphibole (PPL).

Marble

The marble is dominantly whitish with subordinated portions with pink, green, blue and gray shades. The foliation is usually marked by variations in the grain size and by some impurity levels. The marbles can often be folded and may present some coarse to very coarse-grained pockets of recrystallized calcite.

In the thin section, marbles present fine to medium-grained granoblastic texture. They are composed essentially of carbonates–dolomite and subordinated calcite. Exsolution of blebs and lamellae of dolomite can be found in calcite grains. Olivine is rarely found, being partially replaced by tremolite and/or serpentine. Clinopyroxene, phlogopite, scapolite, spinel, talc and humite occur as rare accessory minerals.

Skarns

Two main types of skarns were identified in the study area associated respectively to the metamafic and felsic dykes.

The skarns related to the metamafic bodies are centimeter to decimeter wide; their main mineralogy can be depicted from Fig. 3A. The skarn zones are irregular and enter to the dyke as well as to the marble.

The skarns related to felsic dykes can vary from few millimeters to few centimeters, exceptionally reaching 1.5 m in width (Figs. 3B to 3D). Thinner dykes can be almost completely transformed into skarn (Fig. 3B). The largest skarn studied is composed of distinct mineralogical zones with well-marked or reentrant contacts. A dark green zone classified in the field as exoskarn occurs attached to the marble, and another greyish zone classified as endoskarn occurs attached to the granite (Figs. 3C and 3D).

Skarns associated with metamafic dykes

Two types of skarns, related to amphibolite and hornblende granofels, were selected for a detailed description of the different mineralogical zones.

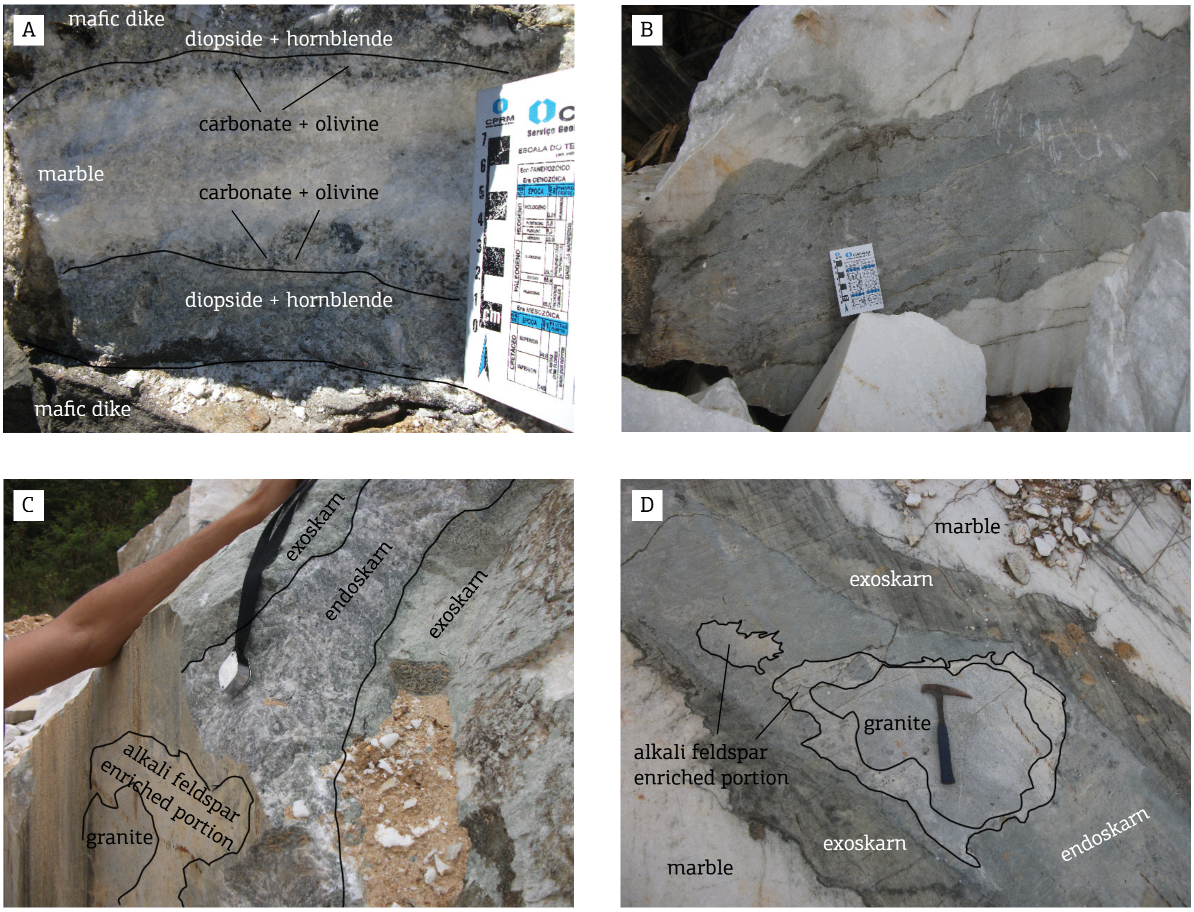

Figure 3. Photographs of the skarns: (A) skarn associated with two metamafic dykes, one on the upper and the other one on the lower portion of the photo (PIES-5); (B) granitic dyke transformed into skarn (PIES-1); (C and D) mineralogical zones associated with the alkali-feldspar granite (PIES-1).

Skarn associated with amphibolites

The skarn associated with the amphibolites dyke has the following mineralogical zones, from marble to amphibolite (Fig. 4A): *carbonate + olivine* and *diopside + hornblende*. These zones are irregular with indentations between them and also with the marble and the dyke.

The *carbonate + olivine* zone is about 1 cm wide and is composed of carbonate (80 to 90 vol%), olivine (10 to 15%) and tremolite (5%), with rare phlogopite. Clinohumite can occur in association with olivine. Carbonate is dolomite and lesser calcite, this last one may present exsolution of blebs of dolomite. Olivine is commonly surrounded by dolomite and tremolite which may be intergrown with vermiform dolomite (Fig. 5A). Replacement by serpentine and iddingsite is common (Figs. 5A and 5B). Olivine is classified as chrysolite (see mineral chemistry). Diopside can occur in this zone surrounding olivine (Fig. 5A), evidencing the infiltration of silica during the skarn generation.

The *diopside + hornblende* zone is about 1.5 cm wide, being composed of diopside (35 to 80 vol%), amphibole (10 to 20%) and carbonate (10 to 40%). Phlogopite reaches up to 5%, apatite and titanite are accessory minerals. Diopside (Fig. 5C) occurs as poikiloblastic grains with inclusions of carbonate, actinolite and phlogopite, and smaller granoblastic grains as inclusions in hornblende. Amphibole (Fig. 5D) is pleochroic in shades of bluish green-brownish green-yellowish and brown that become more intense closer to the amphibolite. Commonly, the grains have compositional zoning (Fig. 5D) with strongly pleochroic cores of Mg-hornblende and edenite, and weakly pleochroic borders of actinolite (see mineral chemistry). Carbonate occurs as inclusion, as well as dispersed between the other minerals.

Skarn associated with hornblende granofels

The skarn associated with hornblende granofels comprises only one mineralogical zone with few millimeters in width (Fig. 4B): *carbonate + olivine*. This zone is composed of carbonate (80 vol%), olivine (10%), amphibole (5%) and phlogopite and Mg-chlorite (5%). Spinel reaches up less than 1%. Carbonate was identified as dolomite and calcite. Olivine and spinel were formed closer to the marble, while Mg-hornblende, Mg-chlorite and phlogopite occur closer to the dyke. Olivine is xenoblastic and partially altered to serpentine and iddingsite (Fig. 5E) or is partially to totally replaced by tremolite (Fig. 5F) and surrounded by dolomite. Tremolite is commonly intergrown with vermiform dolomite. Spinel (pleonaste, see mineral chemistry) is partially replaced by Mg-chlorite (Fig. 5E). Mg-hornblende, occasionally intergrown with carbonate and Mg-chlorite, is larger near the contact with the dyke (Fig. 5F). Mg-chlorite may constitute radial aggregates (Fig. 5F). Phlogopite is colored in shades of orange. It occurs associated with Mg-chlorite near the dyke contact (Fig. 5H) and with carbonate in the dyke.

Skarn associated with felsic dykes

The skarns associated with the monzogranite and syenogranite dykes are about few millimeters to few centimeters in width. They are composed mainly of diopside and scapolite, sometimes also phlogopite, amphibole, epidote and titanite. Near the marble, the skarn is composed of diopside, which can be replaced by hornblende or colorless amphibole and carbonate. Poikiloblastic amphibole with diopside inclusions can also be found.

The skarns associated with the alkali-feldspar granite are the widest (up to 1.5 m) found in the study area. The detailed description of the skarnitic zones encountered in the sampling site PIES-1 (Figs. 1 and 6) are presented ahead.

From marble to granite, the following mineralogical zones were found: (1) *carbonate + tremolite*, (2) *diopside*, and (3) *scapolite + diopside*. In the contact of zone (3) with the granite, there is an alkali-feldspar enriched portion. The names of the zones refer to the most abundant minerals but other mineral phases may occur.

According to Einaudi *et al.* (1981), Einaudi and Burt (1982) and Meinert (1992), skarns are classified as exoskarns if their protolith is the marble, and endoskarns if the protolith is the igneous rock. In the studied skarn, zones (1) and (2) are exoskarns, and zone (3) is an endoskarn. The identification of the endoskarn was made by field-based observations that showed a gradational boundary of the granite and the *scapolite + diopside* zone (endoskarn) (Figs. 3C and 3D), suggesting a metasomatic transformation of the granite. On the other hand, the contact between the endoskarn and the *diopside* zone is abrupt and probably represents the original contact between the granite and the marble. A mineralogical indication of the endoskarn origin is the presence of zircon inherited from the granite. Other arguments concerning the classification of the studied zones as endo and exoskarns are based on their chemical composition in terms of major, trace and Rare Earth Elements (REE) elements as discussed by Mesquita (2016).

Zone (1) is only centimeter wide and it is composed of carbonate (80 to 99 vol%) and tremolite (1 to 15%), with rare olivine (0 to 5%) and phlogopite. Carbonate (dolomite and calcite) may have inclusions of tremolite, olivine and phlogopite. At the contact with zone (2), calcite commonly contains blebs and lamellae of dolomite. Amphibole is colorless to greenish due to chemical variation. It was identified as tremolite, and actinolite (see mineral chemistry) often

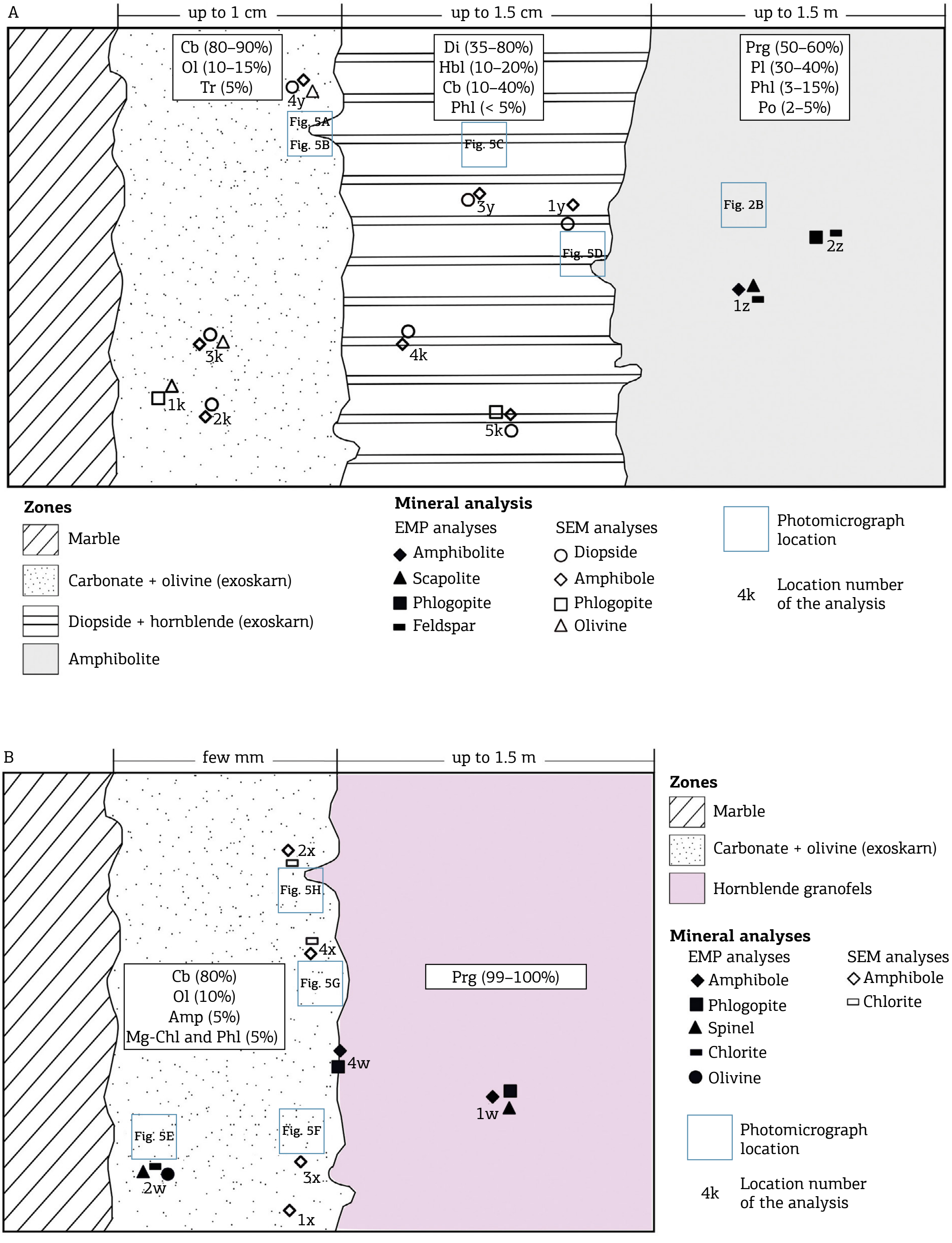

Cb: carbonate; Ol: olivine; Tr: tremolite; Di diopside; Hbl: hornblende; Phl: phlogopite; Prg: pargasite; Pl: plagioclase; Po: pyrrhotite; Amp: amphibole; Mg-Chl: Mg-chlorite; EMP: electron microprobe; SEM: scanning electron microscope.

Figure 4. Illustrative schematic cross-sections (without scale) of the skarns associated with metamafic dykes showing the location of mineral analyses and photomicrographs. The modal mineralogy is indicated within the rectangles. (A) Skarn associated with the amphibolite; (B) skarn associated with the hornblende granofels.

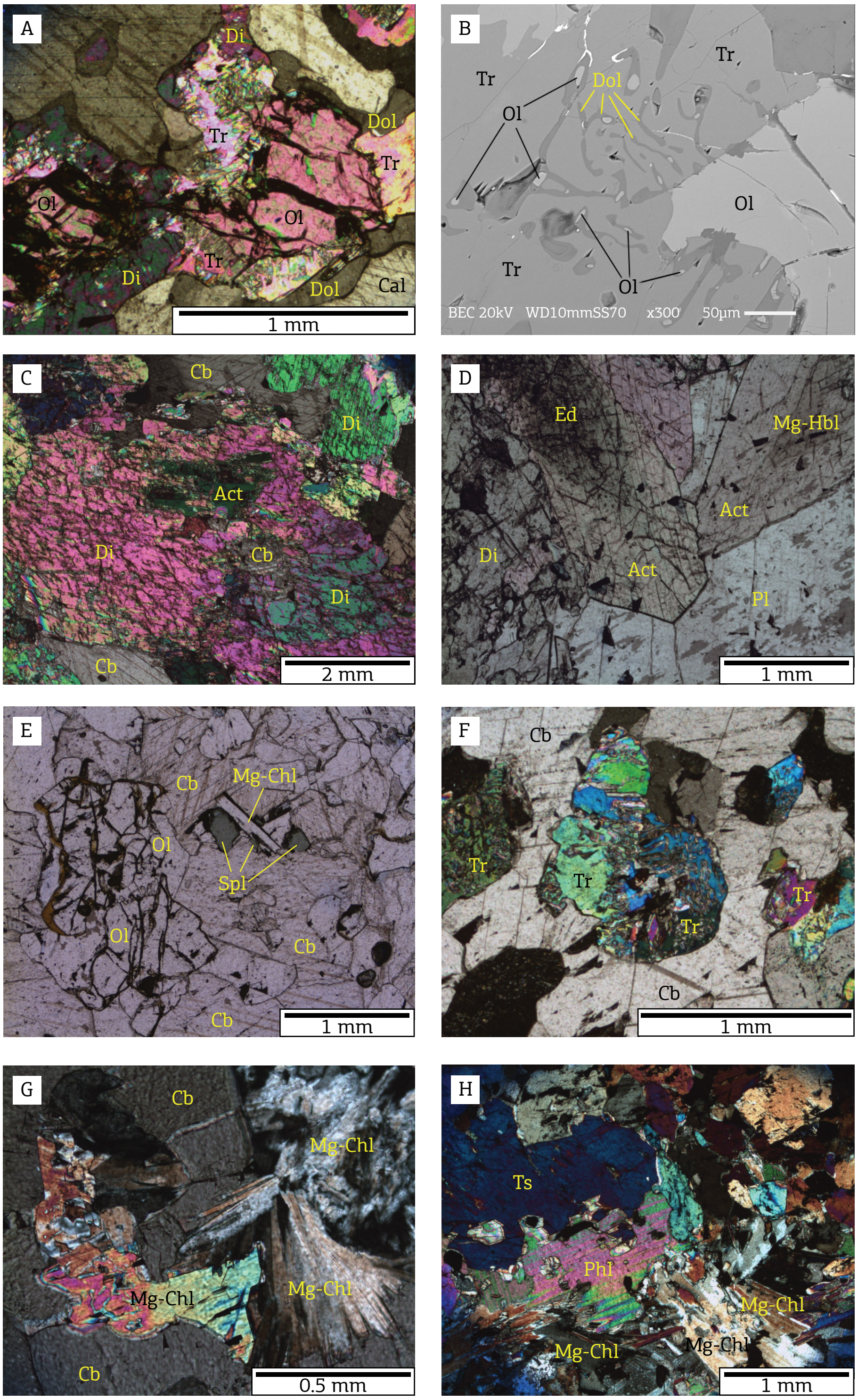

PPL: plane polarized light, XPL: crossed polarizes light.

Figure 5. Photomicrographs and scanning electronic microscope (SEM) image of skarns associated with metamafic dykes. (A) olivine (Ol) replaced by tremolite (Tr) and surrounded by dolomite (Dol) and diopside (Di) (XPL) (PIES-2F1); (B) detailed SEM image of the replacement of olivine by tremolite (PIES-2F1); (C) diopside with replacement by actinolite (Act) and with carbonate (Cb) inclusion (XPL) (PIES-2F1); (D) zoned amphibole with core of edenite (Ed) and Mg-hornblende (Mg-Hbl) and border of actinolite (Act) (PPL) (PIES-2F1); (E) spinel (Spl) grains partially replaced by Mg-chlorite (Mg-Chl) (PPL) (ITA-68A1); (F) tremolite aggregated as pseudomorph after olivine (XPL) (ITA-68A); (G) Mg-hornblende associated with Mg-chlorite (XPL) (ITA-68); (H) skarn border zone with tschermakite (Ts) remnant from the metamafic dyke and neoformed phlogopite (Phl) and Mg-chlorite (XPL) (ITA-68).

displays intergrowths with carbonate (Fig. 7A). Olivine is partially to completely replaced by serpentine. Between zones (1) and (2), there are irregular bands composed of carbonates and amphibole and/or phlogopite (Figs. 7A and 7B).

Zone (2) is up to 1 m wide and it is composed of diopside (up to 95% in volume), accompanied by up to 30% of actinolite (see mineral chemistry) and minor quantities of phlogopite, quartz, zoisite/clinozoisite, carbonate and titanite. Diopside (see mineral chemistry) is found either as larger prismatic or smaller granoblastic grains that occur as inclusions in clinoamphibole (Fig. 7C). The larger grains may be partially replaced by carbonate. Actinolite is poikiloblastic with inclusions of carbonate and diopside (Fig. 7C). Quartz and carbonate occur disseminated among the other minerals (Fig. 7C). At the border of carbonate veins found in this zone, a phlogopite-rich trail was formed (Figs. 6 and 7D). This band is also observed between zones (2) and (3) (Fig. 7E).

Zone (3) is about 0.5 m wide and it is composed of scapolite (50 to 80 vol%) and pyroxene (20 to 50%), with minor quantity of phlogopite. Zircon, zoisite/clinozoisite and colorless clinoamphibole may also occur. The occurrence of zircon in this zone could indicate that its protolith is the alkali-feldspar granite. Zoisite/clinozoisite is more common near zone (2), and actinolite (see mineral chemistry) occurs at the contact with the granite. The texture is granoblastic, characterized by the granular and decussated grains of scapolite, clinopyroxene and lamellar phlogopite (Fig. 7F). Scapolite has

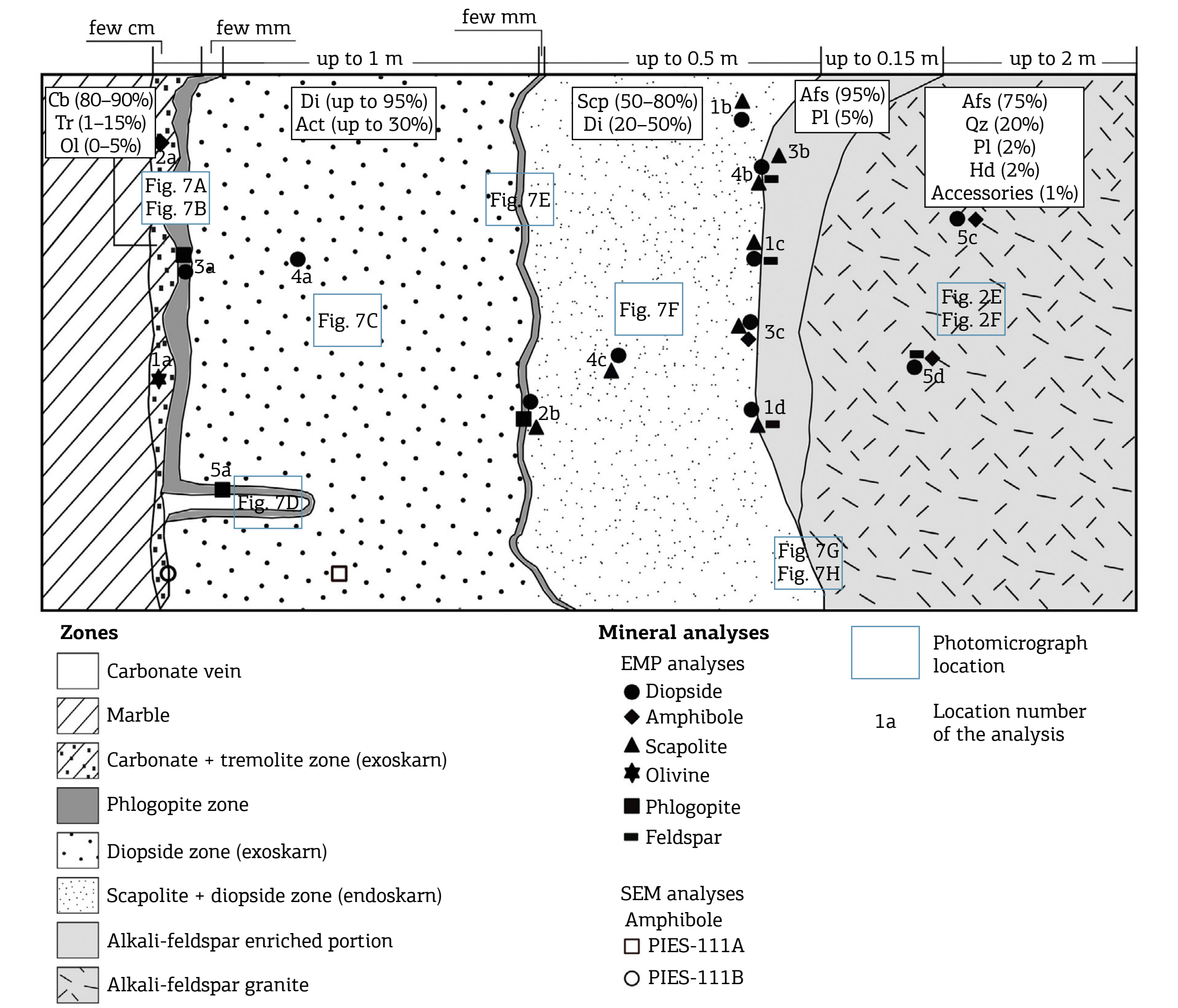

Cb: carbonate; Tr: tremolite; Ol: olivine; Di: diopside; Act: actinolite; Scp: scapolite; Afs: alkali-feldspar; Pl: plagioclase; Qz: quartz; Hd: hedenbergite; EMP: electron microprobe; SEM: scanning electronicmicroscopy.

Figure 6. Illustrative schematic cross-section (without scale) of the skarn associated with alkali-feldspar granite showing the locations of mineral analyses and photomicrographs. The modal mineralogy is indicated within the rectangles.

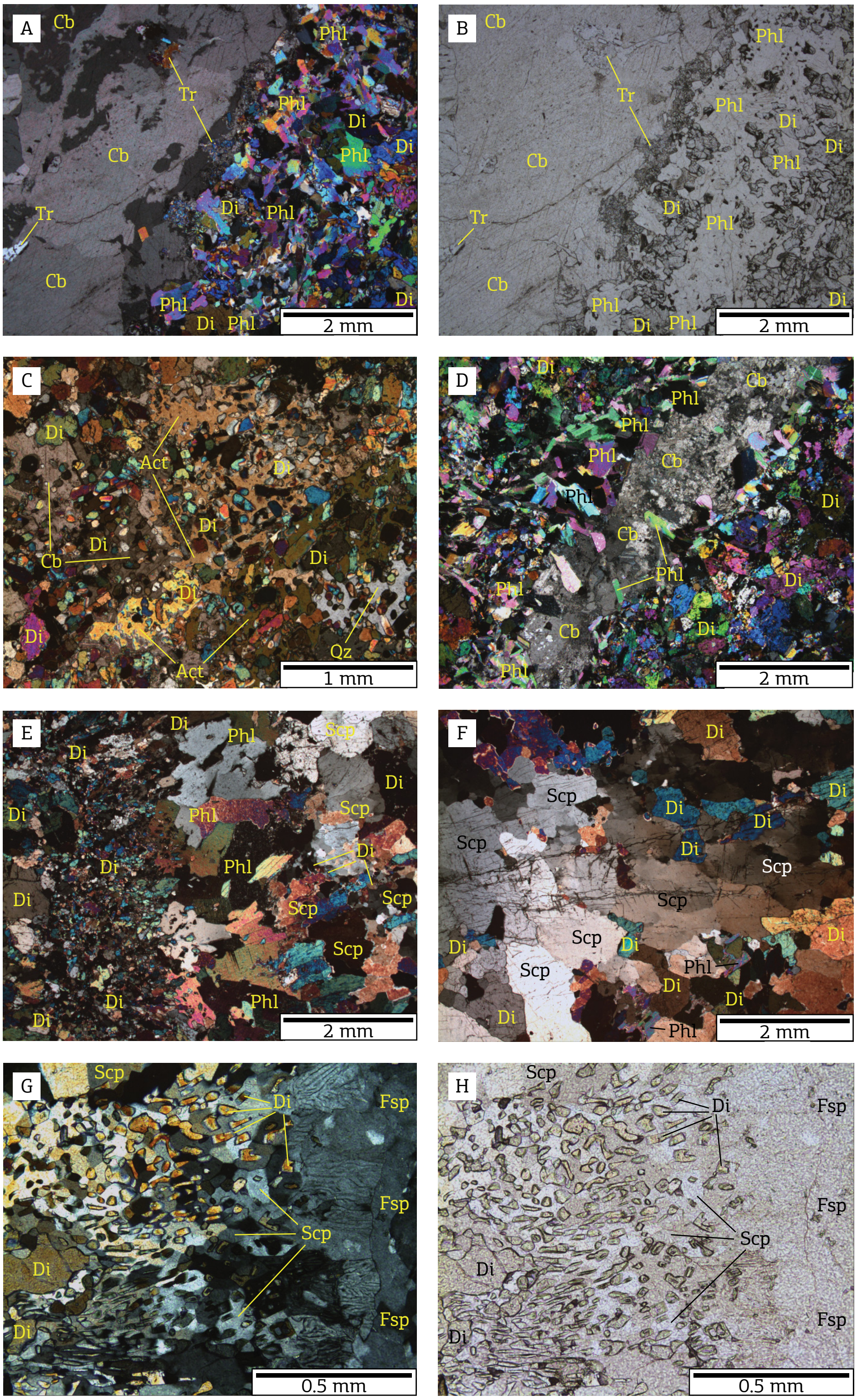

PPL: plane polarized light, XPL: crossed polarizes light.

Figure 7. Photomicrographs of skarns associated with felsic dykes. (A and B) phlogopite (Phl) enriched contact between zones (1) and (2) (left: PPL; right XPL) (ESC +); (C) zone (2) showing poikiloblastic actinolite (Act) with inclusions of diopside (Di) (XPL) (PIES-1-I1A); (D carbonate (Cb) vein bordered by phlogopite seam (XPL) (ESC...); (E) phlogopite-rich contact between zones (2) and (3) (XPL) (CAS29D2); (F) zone (3) with diopside, phlogopite and fractured scapolite (Scp) (XPL) (PIES-1QC); (G and H) contact between zone (3) and granite showing symplectites of diopside intergrown with scapolite (left: PPL; right XPL) (ESC.).

inclusions of carbonate, pyroxene and epidote. It commonly shows undulatory extinction, subgrains and new grains surrounding larger crystals, similar to core-mantle microstructure. Compositional zoning in scapolite is suggested by differences in the birefringence, lower in the core (higher content of sodium) and higher at the border (higher content of calcium). Near the contact with the dyke, scapolite constitutes elongated porphyroblasts grown perpendicularly to the contact or as radial aggregates. This scapolite grains are intergrown with symplectitic diopside (Figs. 7G and 7H) that shows granoblastic texture farther away of the contact with the granite. Scapolite, diopside and zoisite/clinozoisite commonly occur partially replaced by carbonate.

The granite close to the skarn presents an up to 15 cm wide zone rich in alkali-feldspar, which decreases in quantity farther away of the contact distance due to the increase of quartz and plagioclase. The mafic minerals in the granite such as hedenbergite, hastingsite (see mineral chemistry) and biotite occur in minor quantity.

Mineral chemistry

The main minerals of the skarns were analyzed by electron microprobe (EMP) in order to determinate the formula unit and to verify the compositional variations. In addition, analyses were performed by scanning electronic microscopy (SEM) coupled with energy dispersive spectrometer (EDS).

Pyroxene, amphibole, scapolite, olivine, phlogopite, spinel, chlorite and feldspars were analyzed. Tables 1 to 7 show the results of the EMP and SEM analyses and the mineral formulas. Figures 8 and 9 present the classification diagrams obtained for the SEM analyses. The location of the analyzed minerals in the skarnitic zones are shown in Figures 4 and 6.

Pyroxene

The clinopyroxene is the most abundant mineral of the skarns and belongs to the diopside-hedenbergite solid solution. In the skarnitic zones, it is diopside, while in the alkali-feldspar granite it is hedenbergite (Table 1).

Some diopside analyses from the skarnitic zone associated with the amphibolites plotted above of the diopside-hedenbergite series field (Fig. 8A), possibly due to calcium derived from carbonate inclusions. In the *diopside + hornblende zone*, the diopside tends to have more Fe, with X_{Mg} values ranging from 0.76 to 0.90, and less rich in Fe in the *carbonate + olivine* zone, where X_{Mg} ranges from 0.92 to 0.95 (Table 1).

The diopside composition also varies along the skarnitic zone associated with the alkali-feldspar granite. For instance, in the samples ESC and CAS29Pb, diopside is more depleted in Mg in the *scapolite + diopside* zone closer to the granite (X_{Mg}0.77 – 0.95) than in the diopside zone closer to the marble (X_{Mg}0.93 – 0.97, Table 1).

Amphibole

The amphiboles belong to the calcic clinoamphiboles series (Tables 2 and 3). They occur in the skarns associated with both metamafic and felsic dykes, as well as in the granitoids and amphibolites.

In the skarns associated with the amphibolite, there is a compositional variation with increase in Mg and decrease in Fe from the *diopside + hornblende* zone to the *carbonate + olivine* zone. In the *carbonate + olivine* zone, tremolite replaces olivine and diopside while in the other zone actinolite occurs as replacement of diopside (Table 2 and Fig. 8B). These replacements are more likely to be the result of a posterior retrometamorphic process with introduction of aqueous fluid.

In the *diopside + hornblende* zone, amphibole presents compositional zoning, from Mg-hornblende and edenite (core) to actinolite (border) (Figs. 8B and 8C). These zoned grains present a core more enriched in Al, Na and K (Figs. 8D to 8F), with stronger pleochroism, and a border more enriched in Mg (Fig. 8G), with weaker pleochroism. The amphibole of the amphibolite is pargasite (Table 3).

In the skarns associated with the hornblende granofels (sample ITA-68, Fig. 8B, Table 2) tremolite occurs as replacement of olivine in the portions closer to the marble, while Mg-hornblende occurs next to the contact with the mafic dyke. The main amphibole of the hornblende granofels is pargasite (Tables 2 and 3), but tschermakite also occurs (Fig. 8B).

There is a compositional variation in the amphiboles from the mineralogical zones of the skarn related to the alkali-feldspar granite, with an increase of Mg and decrease of Fe toward the marble. The *carbonate + tremolite* zone, closer to the marble, has Mg-rich tremolite (X_{Mg} = 0.99 – 1.00, Table 3) while the *diopside* zone has actinolite (Fig. 8H) with X_{Mg} = 0.76 – 0.77 (Table 2), thus more depleted in Mg.

At the contact between the zones *carbonate + tremolite* and *diopside*, amphibole grains can show compositional variation from tremolite to actinolite (Fig. 8H) as it is indicated by differences in color, from colorless to green. The *scapolite + diopside* zone contains actinolite in the contact with the granite where ranges from 0.80 to 0.85 (Table 3).

In the alkali-feldspar granite, the amphibole occurs as a replacement of hedenbergite. The compositions are Fe-actinolite and Fe-hornblende, with X_{Mg} = 0.40, and hastingsite, with X_{Mg} = 0.18 – 0.21 (Table 3).

Scapolite

Scapolite was classified as dipyre and mizzonite, intermediary members of the marialite-meionite series (Fig. 9A).

In the amphibolites, scapolite occurs as a replacement of plagioclase and is classified as mizzonite with a meionite (Me) component of 66 to 72 mol%.

Table 1. Chemical composition (weight %) of selected diopside and its cationic distribution.

	Pyroxene	Zone	Location	Spot	Mineral	SiO_2	TiO_2	Al_2O_3	FeOt*	MgO	MnO	CaO	Na_2O	K_2O	Total	TSi	TAl	M1Al	M1Ti	$M1Fe^{2+}$	M1Mg	$M2Fe^{2+}$	M2Mn	M2Ca	M2Na	M2K	Cations	*X_{Mg}
Skarn related to the felsic dykes	ESC... (EMP)	diopside	3a	5	Di	52.27	0.19	1.97	1.69	16.67	0.11	26.24	0.23	0.01	99.40	1.91	0.08	0.00	0.01	0.05	0.91	0.00	0.00	1.03	0.02	0.00	4.00	0.94
				6		50.75	0.02	1.57	2.28	16.62	0.06	25.94	0.23	0.00	97.55	1.89	0.07	0.00	0.00	0.07	0.92	0.00	0.00	1.03	0.02	0.00	4.00	0.93
				7		53.48	0.13	1.04	1.25	17.24	0.00	25.98	0.16	0.02	99.29	1.95	0.05	0.00	0.00	0.04	0.94	0.00	0.00	1.02	0.01	0.00	4.00	0.96
				8		54.36	0.00	0.13	0.93	17.91	0.04	26.73	0.09	0.00	100.24	1.96	0.01	0.00	0.00	0.03	0.96	0.00	0.00	1.03	0.01	0.00	4.00	0.97
			4a	1		54.94	0.12	1.19	1.92	16.57	0.12	24.98	0.20	0.01	100.14	2.00	0.00	0.05	0.00	0.05	0.90	0.01	0.00	0.97	0.01	0.00	4.00	0.93
				2		54.27	0.08	1.82	1.68	16.44	0.06	24.91	0.25	0.02	99.72	1.98	0.02	0.06	0.00	0.05	0.89	0.01	0.00	0.97	0.02	0.00	4.00	0.94
				3		55.01	0.08	1.49	1.59	16.80	0.01	25.34	0.23	0.03	100.62	1.99	0.02	0.05	0.00	0.05	0.90	0.00	0.00	0.98	0.02	0.00	4.00	0.95
				4		54.69	0.05	1.54	1.88	16.85	0.06	25.82	0.26	0.00	101.16	1.96	0.04	0.03	0.00	0.06	0.90	0.00	0.00	0.99	0.02	0.00	4.00	0.94
	Esc+++ (EMP)	scapolite + diopside	1b	1	Di	54.18	0.09	1.14	2.58	16.39	0.12	26.20	0.37	0.00	101.09	1.95	0.05	0.00	0.00	0.08	0.88	0.00	0.00	1.01	0.03	0.00	4.00	0.91
				2		53.85	0.08	0.72	2.67	16.38	0.13	26.14	0.26	0.00	100.29	1.96	0.03	0.00	0.00	0.08	0.89	0.00	0.00	1.02	0.02	0.00	4.00	0.91
				3		53.00	0.00	0.49	6.51	13.69	0.31	24.55	0.30	0.03	98.92	1.99	0.01	0.01	0.00	0.20	0.77	0.00	0.01	0.99	0.02	0.00	4.00	0.78
				4		54.29	0.04	0.33	6.23	14.53	0.20	25.28	0.31	0.00	101.22	1.99	0.01	0.00	0.00	0.19	0.79	0.00	0.01	0.99	0.02	0.00	4.00	0.80
			2b	4		54.47	0.09	1.11	1.51	17.31	0.00	26.32	0.21	0.00	101.15	1.95	0.05	0.00	0.00	0.05	0.93	0.00	0.00	1.01	0.01	0.00	4.00	0.95
				5		53.59	0.04	0.76	3.25	15.85	0.23	25.74	0.29	0.01	99.74	1.96	0.03	0.00	0.00	0.10	0.87	0.00	0.01	1.01	0.02	0.00	4.00	0.89
				6		54.72	0.00	1.02	1.61	17.28	0.07	25.92	0.28	0.01	100.98	1.96	0.04	0.01	0.00	0.05	0.93	0.00	0.00	1.00	0.02	0.00	4.00	0.95
				7		53.99	0.00	1.14	1.85	17.05	0.07	25.81	0.26	0.00	100.18	1.95	0.05	0.00	0.00	0.06	0.92	0.00	0.00	1.00	0.02	0.00	4.00	0.94
			4b	4		55.03	0.00	0.26	3.61	16.67	0.07	26.24	0.22	0.01	102.12	1.97	0.01	0.00	0.00	0.11	0.89	0.00	0.00	1.01	0.02	0.00	4.00	0.89
				5		54.86	0.08	0.26	3.24	16.63	0.14	26.14	0.20	0.00	101.56	1.97	0.01	0.00	0.00	0.10	0.89	0.00	0.00	1.01	0.01	0.00	4.00	0.90
				6		54.50	0.02	0.24	3.32	16.51	0.09	25.84	0.23	0.01	100.83	1.98	0.01	0.00	0.00	0.10	0.89	0.00	0.00	1.00	0.02	0.00	4.00	0.90
	CAS29Pb (EMP)	scapolite + diopside	1c	4	Di	53.51	0.00	0.54	4.94	15.08	0.17	24.71	0.37	0.00	99.33	1.98	0.02	0.00	0.00	0.15	0.83	0.00	0.01	0.98	0.03	0.00	4.00	0.84
				5		53.75	0.01	0.53	4.81	14.90	0.13	24.69	0.36	0.00	99.20	1.99	0.01	0.02	0.00	0.15	0.82	0.00	0.00	0.98	0.03	0.00	4.00	0.84
				6		54.13	0.00	0.58	4.63	15.17	0.10	24.55	0.38	0.02	99.57	2.00	0.00	0.02	0.00	0.14	0.83	0.00	0.00	0.97	0.03	0.00	4.00	0.85
			3c	5		54.61	0.00	0.42	6.96	13.63	0.33	25.36	0.33	0.00	101.68	2.00	0.00	0.02	0.00	0.21	0.74	0.00	0.01	0.99	0.02	0.00	4.00	0.77
				6		54.22	0.00	0.36	4.89	15.15	0.12	25.54	0.30	0.00	100.60	1.98	0.02	0.00	0.00	0.15	0.83	0.00	0.00	1.00	0.02	0.00	4.00	0.84
				7		54.74	0.00	0.35	4.70	15.10	0.10	25.24	0.32	0.01	100.57	2.00	0.00	0.02	0.00	0.14	0.82	0.00	0.00	0.99	0.02	0.00	4.00	0.85
			4c	1		55.32	0.05	0.84	2.60	16.19	0.17	26.10	0.23	0.01	101.50	1.99	0.01	0.03	0.00	0.08	0.87	0.00	0.01	1.01	0.02	0.00	4.00	0.91
				2		54.27	0.11	1.08	2.63	16.22	0.12	25.14	0.28	0.00	99.86	1.98	0.02	0.03	0.00	0.08	0.88	0.00	0.00	0.98	0.02	0.00	4.00	0.91
				3		55.17	0.04	1.32	2.36	16.16	0.21	26.04	0.27	0.00	101.60	1.98	0.02	0.04	0.00	0.07	0.87	0.00	0.01	1.00	0.02	0.00	4.00	0.92
		granite	5c	1	Hd	49.40	0.16	1.22	24.64	2.28	1.18	21.33	0.99	0.00	101.24	1.96	0.04	0.02	0.01	0.82	0.14	0.00	0.04	0.91	0.08	0.00	4.00	0.14
				2		48.32	0.01	1.35	25.52	2.09	1.01	21.23	0.99	0.00	100.52	1.94	0.06	0.00	0.00	0.86	0.12	0.00	0.03	0.91	0.08	0.00	4.00	0.12
				3		49.34	0.17	1.34	24.41	2.73	1.15	21.46	1.00	0.00	101.62	1.95	0.05	0.01	0.01	0.81	0.16	0.00	0.04	0.91	0.08	0.00	4.00	0.16
	PIES-1B1 (EMP)	scapolite + diopside	1d	1	Di	51.70	0.00	0.76	10.86	11.29	0.20	24.61	0.41	0.00	99.85	1.95	0.03	0.00	0.00	0.34	0.64	0.00	0.01	1.00	0.03	0.00	4.00	0.65
				2		53.44	0.00	0.58	8.82	14.32	0.16	23.28	0.22	0.03	100.98	1.97	0.03	0.00	0.00	0.21	0.79	0.06	0.01	0.92	0.02	0.00	4.00	0.74
				3		51.64	0.12	0.79	11.66	10.71	0.20	24.54	0.53	0.00	100.21	1.95	0.04	0.00	0.00	0.37	0.60	0.00	0.01	0.99	0.04	0.00	4.00	0.62
				4		52.76	0.09	0.58	8.24	13.34	0.11	25.24	0.38	0.00	100.79	1.95	0.03	0.00	0.00	0.26	0.74	0.00	0.00	1.00	0.03	0.00	4.00	0.74
				5		53.21	0.08	0.57	8.30	13.57	0.18	25.12	0.33	0.00	101.51	1.96	0.03	0.00	0.00	0.25	0.74	0.00	0.01	0.99	0.02	0.00	4.00	0.74
				6		53.12	0.00	0.34	6.01	14.55	0.10	25.37	0.24	0.01	99.75	1.97	0.02	0.00	0.00	0.19	0.80	0.00	0.00	1.01	0.02	0.00	4.00	0.81
				7		53.58	0.00	0.31	3.64	16.05	0.00	25.77	0.19	0.01	99.56	1.97	0.01	0.00	0.00	0.11	0.88	0.00	0.00	1.01	0.01	0.00	4.00	0.89
				8		53.56	0.11	0.43	3.05	16.51	0.13	26.08	0.25	0.00	100.14	1.95	0.02	0.00	0.00	0.09	0.90	0.00	0.00	1.02	0.02	0.00	4.00	0.90
				9		52.64	0.04	0.49	8.33	13.13	0.04	25.21	0.30	0.01	100.23	1.96	0.02	0.00	0.00	0.26	0.73	0.00	0.00	1.01	0.02	0.00	4.00	0.74
				10		52.73	0.00	0.45	6.80	14.15	0.09	25.64	0.35	0.00	100.29	1.95	0.02	0.00	0.00	0.21	0.78	0.00	0.00	1.02	0.03	0.00	4.00	0.79
				11		53.68	0.03	0.33	4.15	15.82	0.03	25.94	0.17	0.01	100.18	1.96	0.01	0.00	0.00	0.13	0.86	0.00	0.00	1.02	0.01	0.00	4.00	0.87
		granite		19	Hd	47.68	0.12	1.18	26.75	2.00	1.13	21.40	0.66	0.00	100.96	1.91	0.06	0.00	0.00	0.88	0.12	0.02	0.04	0.92	0.05	0.00	4.00	0.11
				20		47.75	0.15	1.07	25.81	2.16	0.75	22.29	0.68	0.00	100.66	1.92	0.05	0.00	0.00	0.87	0.13	0.00	0.03	0.96	0.05	0.00	4.00	0.13
				21		47.76	0.11	1.18	25.55	1.97	1.05	21.99	0.66	0.00	100.35	1.93	0.06	0.00	0.00	0.86	0.12	0.00	0.04	0.95	0.05	0.00	4.00	0.12
				22		47.08	0.00	1.24	25.14	1.98	0.71	21.85	0.75	0.01	98.81	1.92	0.06	0.00	0.00	0.86	0.12	0.00	0.03	0.96	0.06	0.00	4.00	0.12
			5d	3		48.70	0.00	0.82	19.77	5.61	0.96	22.73	0.62	0.00	99.29	1.93	0.04	0.00	0.00	0.66	0.33	0.00	0.03	0.97	0.05	0.00	4.00	0.33
				4		48.99	0.08	0.85	19.47	6.38	0.86	22.97	0.62	0.02	100.23	1.91	0.04	0.00	0.00	0.63	0.37	0.01	0.03	0.96	0.05	0.00	4.00	0.36
Skarn related to the mafic dykes	PIES-2F1 (SEM)	diopside + hornblende	1y	18	Di	53.18		0.47	6.48	13.92	0.45	25.22	0.28		100.00	1.97	0.02	0.00		0.20	0.77	0.00	0.01	1.00	0.02		4.00	0.78
				19		52.35		0.56	7.39	13.99	0.40	24.96	0.34		99.99	1.94	0.02	0.00		0.23	0.77	0.00	0.01	0.99	0.02		4.00	0.76
				22		53.54			7.32	13.83		25.31			100.00	1.99	0.00	0.00		0.23	0.77	0.00	0.00	1.01	0.00		4.00	0.77
				24		53.63		2.66	5.89	14.96	0.31	22.05	0.49		99.99	1.97	0.03	0.09		0.09	0.82	0.09	0.01	0.87	0.04		4.00	0.81
			3y	12		53.39			6.88	14.32		25.41			100.00	1.98	0.00	0.00		0.21	0.79	0.01	0.00	1.01	0.00		4.00	0.79
		carbonate + olivine	4y	112		54.28		0.55	2.98	17.17	0.24	24.78			100.00	1.98	0.02	0.00		0.07	0.93	0.03	0.01	0.97	0.00		4.00	0.90
				51		54.74		0.46	1.87	17.03		25.89			99.99	1.99	0.01	0.01		0.06	0.92	0.00	0.00	1.01	0.00		4.00	0.94
				52		54.30		0.40	2.42	16.59		25.93	0.35		99.99	1.98	0.02	0.00		0.07	0.90	0.00	0.00	1.01	0.03		4.00	0.92
	PIES-5A1 (SEM)		2k	11		54.51		0.61	2.09	17.19		25.44	0.16		100.00	1.98	0.02	0.01		0.06	0.93	0.00	0.00	0.99	0.01		4.00	0.94
			3k	18		54.25		0.67	1.72	17.21		25.85	0.30		100.00	1.97	0.03	0.00		0.05	0.93	0.00	0.00	1.00	0.02		4.00	0.95
		diopside + hornblende	4k	21		53.88		0.97	3.14	15.86	0.20	25.65	0.30		100.00	1.97	0.03	0.01		0.10	0.86	0.00	0.01	1.00	0.02		4.00	0.89
				33		54.02		0.55	3.10	16.09		25.84	0.40		100.00	1.97	0.02	0.00		0.10	0.88	0.00	0.00	1.01	0.03		4.00	0.90
			5k	12		53.23		1.08	4.12	15.64	0.24	25.40	0.28		99.99	1.95	0.05	0.00		0.13	0.85	0.00	0.01	1.00	0.02		4.00	0.87

*X_{Mg}: Mg/(Mg+Fe+Mn).

Table 2. Chemical composition (weight %) of selected amphibole, obtained by SEM, and its cationic distribution.

Amphibole	PIES-2F1					PIES-5A1					ITA-68A						PIES-1I1A			PIES-1I1B							
Zone	diopside + hornblende					carbonate + olivine			diopside + hornblende		carbonate + olivine					dike	diopside			contact between carbonate + tremolit and diopside zones							
Location	1y				3y	4y	2k	3k	4k	5k	1x	2x	3x	4x		2x	2	3	4	1		2	3		4	5	
Spot	11 (border)	12 (core)	16 (border)	17 (core)	13 (border)	13	12	16	34	13	13	17	13	14	22	11	13	22	11	16	110	24	11	13	11	24	27
Mineral	Act	Mg-Hbl	Act	Ed	Act	Tr	Tr	Tr	Act	Act	Tr	Mg-Hbl	Tr	Mg-Hbl	Tr	Ts	Act			Act	Tr	Tr	Tr	Act	Tr	Tr	Act
SiO_2	54.98	52.48	54.67	47.46	55.95	59.11	59.76	59.33	58.56	57.28	55.87	49.28	59.29	49.26	57.55	47.41	56.01	56.16	56.83	56.67	58.97	58.86	58.02	56.72	59.60	58.40	55.50
Al_2O_3	2.64	4.90	3.19	10.10	2.27	0.57	0.59	0.99	0.82	2.61	4.43	12.05	1.11	11.79	2.41	14.57	1.59	1.39	0.90	0.92	0.81	1.12	0.94	1.23	0.98	0.91	1.99
FeOt*	10.54	11.21	10.67	13.46	10.13	3.14	2.22	2.55	4.48	5.03	2.78	4.60	2.70		3.13	4.48	10.92	11.45	10.56	10.45	2.67	2.63	4.34	10.23	1.49	3.75	11.05
MgO	17.85	17.19	17.60	14.21	18.24	22.79	23.39	22.78	21.32	20.55	21.68	19.31	23.12	19.23	22.36	18.71	17.90	17.58	18.13	18.55	23.02	23.37	22.15	18.76	23.74	22.43	18.05
MnO	0.27	0.01	0.20														0.32	0.30	0.42	0.18	0.10	0.15	0.25	0.23		0.16	0.29
CaO	13.11	13.24	12.86	12.88	13.40	13.83	14.05	14.03	14.46	13.90	14.21	14.76	13.78	14.10	13.81	14.83	12.55	12.66	12.66	12.88	13.92	13.20	13.85	12.53	13.75	13.84	12.60
Na_2O	0.62	0.98	0.81	1.90		0.39		0.33	0.36	0.63	1.03			1.80	0.74		0.71	0.44	0.50	0.34	0.51	0.67	0.44	0.29	0.43	0.51	0.52
K_2O						0.17																					
Total	100.01	100.01	100	100.01	99.99	100	100.01	100.01	100	100	100	100	100	100	100	100	100	99.98	100	99.99	100	100	99.99	99.99	99.99	100	100
TSi	7.64	7.32	7.60	6.73	7.72	7.97	7.99	7.98	7.98	7.81	7.57	6.64	7.93	6.94	7.77	6.38	7.79	7.81	7.88	7.84	7.94	7.89	7.86	7.81	7.96	7.89	7.69
TAl	0.36	0.68	0.40	1.27	0.28	0.03	0.01	0.02	0.03	0.19	0.43	1.37	0.07	1.06	0.23	1.63	0.22	0.19	0.12	0.14	0.06	0.11	0.15	0.17	0.04	0.11	0.30
TFe^{3+}	0.00	0.00	0.00	0.00	0.00	0.00	0.00	0.00	0.00	0.00	0.00	0.00	0.00	0.00	0.00	0.00	0.00	0.00	0.00	0.02	0.00	0.00	0.00	0.02	0.00	0.00	0.01
Sum T	**8.00**	**8.00**	**8.00**	**8.00**	**8.00**	**8.00**	**8.00**	**8.00**	**8.00**	**8.00**	**8.00**	**8.00**	**8.00**	**8.00**	**8.00**	**8.00**	**8.00**	**8.00**	**8.00**	**8.00**	**8.00**	**8.00**	**8.00**	**8.00**	**8.00**	**8.00**	**8.00**
CAl	0.07	0.13	0.13	0.42	0.09	0.06	0.08	0.14	0.10	0.23	0.28	0.55	0.10	0.90	0.15	0.68	0.05	0.04	0.03	0.01	0.07	0.07	0.01	0.03	0.12	0.04	0.03
CFe^{3+}	0.18	0.31	0.14	0.37	0.21	0.00	0.00	0.00	0.00	0.00	0.00	0.49	0.02	0.00	0.00	0.50	0.17	0.17	0.13	0.16	0.00	0.08	0.02	0.24	0.00	0.00	0.28
CTi	0.00	0.00	0.00	0.00	0.00	0.00	0.00	0.00	0.00	0.00	0.00	0.00	0.00	0.00	0.00	0.00	0.00	0.00	0.00	0.00	0.00	0.00	0.00	0.00	0.00	0.00	0.00
CMg	3.70	3.58	3.65	3.01	3.75	4.58	4.66	4.57	4.33	4.18	4.38	3.88	4.61	4.04	4.50	3.75	3.71	3.65	3.75	3.83	4.62	4.67	4.47	3.85	4.73	4.52	3.73
CFe^{2+}	1.04	0.99	1.07	1.20	0.95	0.35	0.25	0.29	0.51	0.57	0.32	0.03	0.27	0.00	0.35	0.00	1.06	1.13	1.06	1.00	0.30	0.18	0.48	0.86	0.15	0.42	0.95
CMn	0.02	0.00	0.01	0.00	0.00	0.00	0.00	0.00	0.00	0.00	0.00	0.00	0.00	0.00	0.00	0.00	0.02	0.02	0.03	0.01	0.01	0.01	0.03	0.01	0.00	0.02	0.02
CCa	0.00	0.00	0.00	0.00	0.00	0.00	0.01	0.01	0.06	0.02	0.03	0.06	0.00	0.06	0.00	0.06	0.00	0.00	0.00	0.00	0.00	0.00	0.00	0.00	0.00	0.00	0.00
Sum C	**5.00**	**5.00**	**5.00**	**5.00**	**5.00**	**5.00**	**5.00**	**5.00**	**5.00**	**5.00**	**5.00**	**5.00**	**5.00**	**5.00**	**5.00**	**5.00**	**5.00**	**5.00**	**5.00**	**5.00**	**5.00**	**5.00**	**5.00**	**5.00**	**5.00**	**5.00**	**5.00**
BMg	0.00	0.00	0.00	0.00	0.00	0.00	0.00	0.00	0.00	0.00	0.00	0.00	0.00	0.00	0.00	0.00	0.00	0.00	0.00	0.00	0.00	0.00	0.00	0.00	0.00	0.00	0.00
BFe^{2+}	0.01	0.01	0.03	0.02	0.01	0.00	0.00	0.00	0.00	0.00	0.00	0.00	0.01	0.00	0.00	0.00	0.04	0.04	0.03	0.03	0.00	0.04	0.00	0.06	0.02	0.00	0.04
BMn	0.02	0.00	0.01	0.00	0.00	0.00	0.00	0.00	0.00	0.00	0.00	0.00	0.00	0.00	0.00	0.00	0.02	0.02	0.03	0.01	0.00	0.01	0.00	0.01	0.00	0.00	0.02
BCa	1.95	1.98	1.92	1.96	1.98	2.00	2.00	2.00	2.00	2.00	2.00	2.00	1.97	2.00	2.00	2.00	1.87	1.89	1.88	1.91	2.00	1.90	2.00	1.85	1.97	2.00	1.87
BNa	0.03	0.01	0.05	0.02	0.00	0.00	0.00	0.00	0.00	0.00	0.00	0.00	0.00	0.00	0.00	0.00	0.07	0.06	0.06	0.05	0.00	0.06	0.00	0.04	0.02	0.00	0.07
Sum B	**2.00**	**2.00**	**2.00**	**2.00**	**1.99**	**2.00**	**2.00**	**2.00**	**2.00**	**2.00**	**2.00**	**2.00**	**1.99**	**2.00**	**2.00**	**2.00**	**2.00**	**2.00**	**2.00**	**2.00**	**2.00**	**2.00**	**2.00**	**1.96**	**2.00**	**2.00**	**2.00**
ACa	0.00	0.00	0.00	0.00	0.00	0.00	0.01	0.01	0.06	0.02	0.03	0.07	0.00	0.07	0.00	0.07	0.00	0.00	0.00	0.00	0.00	0.00	0.01	0.00	0.00	0.00	0.00
ANa	0.14	0.25	0.17	0.50	0.00	0.10	0.00	0.09	0.10	0.17	0.27	0.00	0.00	0.49	0.19	0.00	0.12	0.06	0.07	0.05	0.13	0.12	0.12	0.04	0.10	0.13	0.07
AK	0.00	0.00	0.00	0.00	0.00	0.03	0.00	0.00	0.00	0.00	0.00	0.00	0.00	0.00	0.00	0.00	0.00	0.00	0.00	0.00	0.00	0.00	0.00	0.00	0.00	0.00	0.00
Sum A	**0.14**	**0.25**	**0.17**	**0.50**	**0.00**	**0.13**	**0.01**	**0.10**	**0.15**	**0.18**	**0.30**	**0.07**	**0.00**	**0.56**	**0.19**	**0.07**	**0.12**	**0.06**	**0.07**	**0.05**	**0.14**	**0.12**	**0.12**	**0.04**	**0.10**	**0.14**	**0.07**
Cations	15.14	15.25	15.17	15.50	14.99	15.13	15.01	15.10	15.16	15.18	15.30	15.07	14.99	15.56	15.19	15.07	15.12	15.06	15.07	15.04	15.14	15.12	15.12	15.00	15.10	15.14	15.07
CCl	0.00	0.00	0.00	0.00	0.00	0.00	0.00	0.00	0.00	0.00	0.00	0.00	0.00	0.00	0.00	0.00	0.00	0.00	0.00	0.00	0.00	0.00	0.00	0.00	0.00	0.00	0.00
CF	0.00	0.00	0.00	0.00	0.00	0.00	0.00	0.00	0.00	0.00	0.00	0.00	0.00	0.00	0.00	0.00	0.00	0.00	0.00	0.00	0.00	0.00	0.00	0.00	0.00	0.00	0.00
Sum O	**23.00**	**23.00**	**23.00**	**23.00**	**23.00**	**23.08**	**23.04**	**23.11**	**23.15**	**23.12**	**23.09**	**22.91**	**23.01**	**23.24**	**23.05**	**22.85**	**23.02**	**23.01**	**23.03**	**23.00**	**23.07**	**23.05**	**23.00**	**23.00**	**23.08**	**23.03**	**23.00**
$*X_{Mg}$	0.78	0.78	0.77	0.71	0.80	0.93	0.95	0.94	0.89	0.88	0.93	0.99	0.94	1.00	0.93	1.00	0.77	0.76	0.77	0.79	0.94	0.96	0.90	0.81	0.97	0.91	0.79

$*X_{Mg}$: $Mg/(Mg+Fe^{2+})$.

Table 3. Chemical composition (weight %) of selected amphibole, obtained by electron microprobe (EMP), and its cationic distribution.

Amphibole	ITA-68A1						PIES-5F1						ESC...			CAS29Pb							PIES-1B1	
Zone	hornblende granofels			contact between skarn and dike			amphibolite						carbonate + tremolite			scapolite + diopside			granite					
Location	1w			4w			1z						2a			3c			5c				5d	
Spot	2	5	6	4	5	6	1	2	3	4	5	6	1	2	3	1	4	8	4	5	6	7	1	2
Mineral	Prg						Prg						Tr			Act			Hst				Fe-Act	Fe-Hbl
SiO_2	45.02	46.41	45.39	45.17	45.52	44.60	43.93	46.07	45.74	43.96	44.93	43.45	57.07	56.65	57.48	56.63	57.36	55.87	38.58	38.09	36.45	38.72	49.54	47.30
TiO_2	0.76	1.15	0.86	1.24	1.34	1.20	1.08	1.26	1.35	1.56	1.10	1.24	0.12	0.00	0.00	0.01	0.05	0.17	0.36	0.20	0.37	0.15	0.04	0.12
Al_2O_3	14.19	13.85	13.59	14.87	14.38	14.64	14.25	13.62	13.86	15.07	13.81	15.07	0.57	0.69	0.52	1.23	1.06	1.92	11.29	11.64	10.92	11.31	2.65	4.68
FeOt*	3.56	3.30	3.74	3.61	3.48	3.38	7.65	7.48	7.20	7.75	8.04	7.65	0.26	0.33	0.28	6.58	6.32	8.53	29.22	29.74	29.31	29.39	23.30	24.46
MgO	17.56	17.82	17.82	17.31	17.63	17.60	15.27	15.51	15.35	14.53	15.21	14.45	23.99	24.16	24.14	19.68	19.51	18.36	3.17	2.87	3.24	3.02	8.04	7.51
MnO	0.01	0.01	0.03	0.07	0.01	0.03	0.10	0.18	0.06	0.13	0.12	0.12	0.00	0.08	0.10	0.04	0.18	0.14	0.86	0.89	0.65	0.72	1.15	1.13
CaO	13.05	13.31	13.39	13.37	13.38	13.21	12.70	12.87	12.93	13.03	13.05	12.70	13.52	13.45	13.68	13.27	13.50	12.64	11.22	11.46	10.96	11.39	11.75	11.64
Na_2O	1.59	1.69	1.55	1.85	1.68	1.72	1.77	1.83	1.90	1.90	1.83	1.98	0.35	0.36	0.26	0.29	0.18	0.49	1.55	1.33	1.42	1.46	0.38	0.50
K_2O	1.08	0.81	0.84	0.85	0.95	0.89	1.08	1.09	1.09	1.25	1.11	1.28	0.21	0.24	0.18	0.12	0.11	0.20	2.31	2.56	2.21	2.32	0.17	0.41
F	0.41	0.61	0.36	0.10	0.62	0.73	0.42	0.66	0.46	0.26	0.25	0.41	0.47	0.93	0.35	0.31	0.15	0.30	0.26	0.01	0.05	0.00	0.28	0.00
Cl	0.07	0.07	0.07	0.08	0.07	0.08	0.21	0.17	0.21	0.27	0.19	0.23	0.00	0.00	0.00	0.02	0.02	0.01	1.99	2.24	2.03	2.08	0.03	0.07
Total	**97.30**	**99.01**	**97.64**	**98.52**	**99.06**	**98.08**	**98.46**	**100.72**	**100.14**	**99.69**	**99.64**	**98.56**	**96.57**	**96.88**	**96.99**	**98.18**	**98.44**	**98.63**	**100.80**	**101.04**	**97.61**	**100.54**	**97.33**	**97.81**
TSi	6.40	6.49	6.42	6.35	6.38	6.31	6.30	6.48	6.47	6.27	6.39	6.27	7.91	7.85	7.91	7.92	8.00	7.85	6.13	6.06	5.98	6.16	7.59	7.22
TAl	1.60	1.51	1.58	1.66	1.62	1.69	1.70	1.52	1.53	1.73	1.62	1.73	0.09	0.11	0.09	0.08	0.00	0.15	1.87	1.94	2.02	1.84	0.42	0.78
TFe3	0.00	0.00	0.00	0.00	0.00	0.00	0.00	0.00	0.00	0.00	0.00	0.00	0.00	0.04	0.00	0.00	0.00	0.00	0.00	0.00	0.00	0.00	0.00	0.00
TTi	0.00	0.00	0.00	0.00	0.00	0.00	0.00	0.00	0.00	0.00	0.00	0.00	0.01	0.00	0.00	0.00	0.00	0.00	0.00	0.00	0.00	0.00	0.00	0.00
Sum T	**8.00**	**8.00**	**8.00**	**8.00**	**8.00**	**8.00**	**8.00**	**8.00**	**8.00**	**8.00**	**8.00**	**8.00**	**8.01**	**8.00**	**8.00**	**8.00**	**8.00**	**8.00**	**8.00**	**8.00**	**8.00**	**8.00**	**8.00**	**8.00**
CAl	0.78	0.78	0.69	0.81	0.76	0.75	0.71	0.74	0.78	0.81	0.70	0.84	0.00	0.00	0.00	0.13	0.17	0.17	0.25	0.24	0.09	0.28	0.06	0.06
CCr	0.00	0.00	0.00	0.00	0.00	0.00	0.00	0.00	0.00	0.00	0.00	0.00	0.00	0.00	0.00	0.00	0.00	0.00	0.00	0.00	0.00	0.00	0.00	0.00
CFe^{3+}	0.04	0.00	0.10	0.00	0.00	0.04	0.12	0.00	0.00	0.00	0.01	0.00	0.00	0.00	0.00	0.00	0.00	0.02	0.68	0.77	1.01	0.66	0.28	0.58
CTi	0.08	0.12	0.09	0.13	0.14	0.13	0.12	0.13	0.14	0.17	0.12	0.13	0.01	0.00	0.00	0.00	0.01	0.02	0.04	0.02	0.05	0.02	0.01	0.01
CMg	3.72	3.72	3.76	3.63	3.69	3.71	3.27	3.25	3.24	3.09	3.22	3.11	4.96	4.99	4.95	4.10	4.06	3.85	0.75	0.68	0.79	0.72	1.83	1.71
CFe^{2+}	0.38	0.38	0.35	0.42	0.41	0.36	0.78	0.86	0.84	0.93	0.95	0.91	0.03	0.00	0.03	0.77	0.74	0.94	3.20	3.18	3.01	3.26	2.71	2.55
CMn	0.00	0.00	0.00	0.01	0.00	0.00	0.01	0.01	0.00	0.01	0.01	0.01	0.00	0.01	0.01	0.00	0.02	0.01	0.07	0.10	0.06	0.07	0.12	0.10
CCa	0.00	0.00	0.01	0.01	0.01	0.00	0.00	0.00	0.00	0.00	0.00	0.00	0.01	0.00	0.01	0.00	0.01	0.00	0.00	0.00	0.00	0.00	0.00	0.00
Sum C	**5.00**	**5.00**	**5.00**	**5.00**	**5.00**	**5.00**	**5.00**	**5.00**	**5.00**	**5.00**	**5.00**	**5.00**	**5.00**	**5.00**	**5.00**	**5.00**	**5.00**	**5.00**	**5.00**	**5.00**	**5.00**	**5.00**	**5.00**	**5.00**
BMg	0.00	0.00	0.00	0.00	0.00	0.00	0.00	0.00	0.00	0.00	0.00	0.00	0.00	0.00	0.00	0.00	0.00	0.00	0.00	0.00	0.00	0.00	0.00	0.00
BFe^{2+}	0.01	0.00	0.00	0.00	0.00	0.00	0.02	0.02	0.02	0.00	0.00	0.01	0.00	0.00	0.00	0.00	0.00	0.04	0.00	0.00	0.00	0.00	0.00	0.00
BMn	0.00	0.00	0.00	0.00	0.00	0.00	0.01	0.01	0.00	0.00	0.01	0.01	0.00	0.00	0.00	0.00	0.00	0.01	0.04	0.02	0.04	0.03	0.03	0.05
BCa	1.99	2.00	2.00	2.00	2.00	2.00	1.95	1.94	1.96	1.99	1.99	1.97	2.00	2.00	2.00	1.99	2.00	1.90	1.91	1.95	1.93	1.94	1.93	1.90
BNa	0.01	0.00	0.00	0.00	0.00	0.00	0.03	0.03	0.02	0.00	0.01	0.02	0.01	0.00	0.00	0.01	0.00	0.05	0.05	0.03	0.04	0.03	0.04	0.05
Sum B	**2.00**	**2.00**	**2.00**	**2.00**	**2.00**	**2.00**	**2.00**	**2.00**	**2.00**	**2.00**	**2.00**	**2.00**	**2.00**	**2.00**	**2.00**	**2.00**	**2.00**	**2.00**	**2.00**	**2.00**	**2.00**	**2.00**	**2.00**	**2.00**
ACa	0.00	0.00	0.02	0.01	0.01	0.00	0.00	0.00	0.00	0.00	0.00	0.00	0.00	0.00	0.01	0.00	0.01	0.00	0.00	0.00	0.00	0.00	0.00	0.00
ANa	0.43	0.46	0.43	0.50	0.46	0.47	0.47	0.47	0.50	0.52	0.50	0.54	0.09	0.09	0.07	0.07	0.05	0.08	0.43	0.39	0.41	0.42	0.07	0.10
AK	0.20	0.14	0.15	0.15	0.17	0.16	0.20	0.20	0.20	0.23	0.20	0.24	0.04	0.04	0.03	0.02	0.02	0.04	0.47	0.52	0.46	0.47	0.03	0.08
Sum A	**0.63**	**0.60**	**0.59**	**0.66**	**0.63**	**0.64**	**0.66**	**0.66**	**0.70**	**0.75**	**0.70**	**0.77**	**0.13**	**0.14**	**0.11**	**0.09**	**0.08**	**0.12**	**0.90**	**0.91**	**0.88**	**0.89**	**0.11**	**0.18**
Cations	15.63	15.60	15.59	15.66	15.63	15.64	15.66	15.66	15.70	15.75	15.70	15.77	15.14	15.14	15.11	15.09	15.08	15.12	15.90	15.91	15.88	15.89	15.11	15.18
CCl	0.02	0.02	0.02	0.02	0.02	0.02	0.05	0.04	0.05	0.07	0.05	0.06	0.00	0.00	0.00	0.01	0.00	0.00	0.54	0.61	0.57	0.56	0.01	0.02
CF	0.19	0.27	0.16	0.04	0.27	0.33	0.19	0.29	0.21	0.12	0.11	0.19	0.21	0.41	0.15	0.14	0.07	0.13	0.13	0.00	0.03	0.00	0.14	0.00
Sum O	**23.00**	**23.06**	**23.00**	**23.04**	**23.03**	**23.00**	**23.00**	**23.06**	**23.11**	**23.08**	**23.01**	**23.06**	**23.03**	**22.99**	**23.01**	**23.07**	**23.14**	**23.07**	**23.00**	**23.00**	**23.00**	**23.00**	**23.00**	**23.00**
$^*X_{Mg}$	0.91	0.91	0.92	0.90	0.90	0.91	0.80	0.79	0.79	0.77	0.77	0.77	0.99	1.00	0.99	0.84	0.85	0.80	0.19	0.18	0.21	0.18	0.40	0.40

$^*X_{Mg}$: $Mg/(Mg+Fe^{2+})$.

Table 4. Chemical composition (weight %) of selected scapolite, obtained by electron microprobe (EMP), and its cationic distribution.

Scapolite	Zone	Location	Spot	SiO_2	TiO_2	Al_2O_3	FeOt*	MgO	MnO	CaO	Na_2O	K_2O	Total	Cl	F	S	Si	Al	Ti	Fe^{2+}	Cr	Mn	Mg	Ca	Na	K	Cátions	Me*
CAS29Pb	Contact between granite and scapolite + diopside zone	1c	1	54.58	0.05	23.72	0.00	0.02	0.06	9.90	7.57	0.65	98.29	2.20	0.06	0.00	7.72	3.95	0.01	0.00	0.00	0.01	0.00	1.50	2.08	0.12	15.39	42
			2	54.34	0.07	23.53	0.00	0.00	0.00	9.76	7.43	0.63	97.68	2.29	0.23	0.01	7.74	3.95	0.01	0.00	0.00	0.00	0.00	1.49	2.05	0.12	15.35	42
			3	53.52	0.00	24.05	0.02	0.00	0.00	10.45	7.20	0.64	97.58	2.07	0.15	0.01	7.64	4.04	0.00	0.00	0.00	0.00	0.00	1.60	1.99	0.12	15.39	45
		3c	9	56.15	0.00	23.39	0.08	0.00	0.00	9.08	8.13	0.67	99.57	2.47	0.11	0.03	7.85	3.85	0.00	0.01	0.00	0.00	0.00	1.36	2.20	0.12	15.39	38
			10	55.30	0.00	23.22	0.03	0.00	0.04	8.79	8.03	0.73	98.09	2.38	0.10	0.02	7.84	3.87	0.00	0.00	0.00	0.01	0.00	1.34	2.21	0.13	15.39	38
			11	56.25	0.00	23.07	0.07	0.00	0.00	8.64	8.37	0.67	99.07	2.53	0.00	0.01	7.89	3.81	0.00	0.01	0.00	0.00	0.00	1.30	2.28	0.12	15.40	36
	scapolite + diopside	4c	4	48.84	0.09	26.45	0.03	0.00	0.00	14.91	4.67	0.50	96.55	1.21	0.13	0.02	7.09	4.52	0.01	0.00	0.00	0.00	0.00	2.32	1.32	0.09	15.34	64
			5	49.50	0.00	26.72	0.00	0.00	0.00	15.30	4.60	0.49	97.72	1.26	0.15	0.02	7.10	4.51	0.00	0.00	0.00	0.00	0.00	2.35	1.28	0.09	15.33	65
			6	49.32	0.03	26.61	0.01	0.00	0.00	15.24	4.49	0.50	97.10	1.17	0.00	0.00	7.10	4.51	0.00	0.00	0.00	0.00	0.00	2.35	1.25	0.09	15.31	65
			7	49.53	0.03	26.50	0.01	0.00	0.00	15.00	4.77	0.49	97.29	1.22	0.00	0.00	7.12	4.49	0.00	0.00	0.00	0.00	0.00	2.31	1.33	0.09	15.34	63
Esc +++	scapolite + diopside	1b	5 (border)	53.14	0.07	25.41	0.00	0.00	0.01	11.14	7.15	0.64	99.26	2.13	0.02	0.01	7.48	4.21	0.01	0.00	0.00	0.00	0.00	1.68	1.95	0.12	15.44	46
			6 (border)	53.47	0.00	25.07	0.00	0.00	0.02	10.90	7.38	0.66	99.31	2.13	0.18	0.02	7.53	4.15	0.00	0.00	0.00	0.00	0.00	1.64	2.01	0.12	15.46	45
			7 (core)	55.33	0.08	24.78	0.04	0.02	0.02	9.48	8.29	0.67	100.44	2.20	0.00	0.02	7.66	4.04	0.01	0.00	0.00	0.00	0.00	1.41	2.23	0.12	15.47	39
			8 (core)	54.99	0.00	23.84	0.05	0.01	0.07	8.99	8.25	0.63	98.86	2.61	0.00	0.01	7.75	3.96	0.00	0.01	0.00	0.01	0.00	1.36	2.26	0.11	15.45	38
			9 (border)	53.91	0.00	24.46	0.03	0.01	0.00	10.24	7.37	0.01	97.77	2.21	0.00	0.01	7.65	4.09	0.00	0.00	0.00	0.00	0.00	1.56	2.03	0.00	15.32	43
			10 (core)	53.91	0.10	24.29	0.04	0.00	0.00	9.25	7.93	0.65	98.07	2.44	0.00	0.01	7.66	4.06	0.01	0.00	0.00	0.00	0.00	1.41	2.18	0.12	15.45	39
			11 (border)	53.27	0.11	24.70	0.05	0.00	0.00	10.44	7.31	0.59	98.18	2.19	0.00	0.01	7.56	4.13	0.01	0.01	0.00	0.00	0.00	1.59	2.01	0.11	15.42	44
			12 (core)	53.52	0.00	24.78	0.07	0.00	0.00	10.37	7.47	0.59	98.52	2.20	0.00	0.01	7.57	4.13	0.00	0.01	0.00	0.00	0.00	1.57	2.05	0.11	15.44	43
	Contact: scapolite + diopside and diopside	2b	7	48.58	0.00	26.41	0.05	0.00	0.00	14.50	5.18	0.51	96.35	1.36	0.00	0.03	7.08	4.53	0.00	0.01	0.00	0.00	0.00	2.26	1.46	0.10	15.43	61
			8	48.61	0.00	26.50	0.02	0.00	0.03	14.92	4.98	0.51	96.70	1.31	0.06	0.03	7.06	4.53	0.00	0.00	0.00	0.00	0.00	2.32	1.40	0.10	15.42	62
			10	49.19	0.00	26.39	0.01	0.00	0.00	14.51	5.42	0.50	97.23	1.41	0.03	0.04	7.10	4.49	0.00	0.00	0.00	0.00	0.00	2.25	1.52	0.09	15.45	60
			11	49.07	0.00	26.02	0.00	0.00	0.01	14.23	5.28	0.50	96.38	1.50	0.04	0.03	7.15	4.46	0.00	0.00	0.00	0.00	0.00	2.22	1.49	0.09	15.41	60
	Contact between granite and scapolite + diopside zone	3b	1	56.26	0.03	23.17	0.02	0.00	0.00	7.54	9.09	0.84	99.21	2.85	0.09	0.00	7.90	3.83	0.00	0.00	0.00	0.00	0.00	1.13	2.47	0.15	15.49	31
			2	55.75	0.00	23.29	0.06	0.00	0.04	7.65	9.12	0.64	98.83	2.84	0.07	0.02	7.86	3.87	0.00	0.01	0.00	0.01	0.00	1.16	2.49	0.12	15.51	32
			3	56.51	0.00	23.71	0.03	0.00	0.01	8.03	8.79	0.74	100.14	2.80	0.17	0.03	7.86	3.88	0.00	0.00	0.00	0.00	0.00	1.20	2.37	0.13	15.44	34
			4	55.20	0.00	23.04	0.01	0.01	0.02	7.83	8.66	0.80	97.74	2.78	0.00	0.01	7.86	3.87	0.00	0.00	0.00	0.00	0.00	1.20	2.39	0.15	15.47	33
		4b	1	56.60	0.12	22.91	0.00	0.00	0.02	7.58	8.98	0.93	99.39	2.76	0.15	0.01	7.93	3.78	0.01	0.00	0.00	0.00	0.00	1.14	2.44	0.17	15.47	32
			2	57.33	0.00	22.24	0.03	0.00	0.05	6.47	9.61	0.96	99.07	3.07	0.00	0.00	8.05	3.68	0.00	0.00	0.00	0.01	0.00	0.97	2.62	0.17	15.50	27
			3	55.47	0.00	23.47	0.09	0.01	0.00	8.11	8.84	0.67	98.92	2.80	0.13	0.01	7.82	3.90	0.00	0.01	0.00	0.00	0.00	1.23	2.42	0.12	15.49	34
PIES-1B1		1d	12	53.43	0.05	23.38	0.01	0.00	0.04	9.08	8.23	0.67	96.81	2.45	0.00	0.01	7.70	3.97	0.01	0.00	0.00	0.01	0.00	1.40	2.30	0.12	15.51	38
			13	52.97	0.10	23.34	0.05	0.05	0.00	8.88	8.16	0.67	96.19	2.54	0.00	0.00	7.69	3.99	0.01	0.01	0.00	0.00	0.01	1.38	2.30	0.12	15.51	38
			14	53.43	0.03	23.32	0.08	0.00	0.00	9.20	8.09	0.74	96.87	2.47	0.11	0.00	7.71	3.96	0.00	0.01	0.00	0.00	0.00	1.42	2.26	0.14	15.50	39
			15	53.42	0.01	23.63	0.10	0.00	0.00	9.55	7.67	0.69	96.88	2.32	0.00	0.00	7.69	4.00	0.00	0.01	0.00	0.00	0.00	1.47	2.14	0.13	15.44	41
			16	54.16	0.03	23.42	0.04	0.00	0.00	8.96	8.05	0.62	97.12	2.36	0.00	0.01	7.76	3.95	0.00	0.00	0.00	0.00	0.00	1.38	2.23	0.11	15.43	38
			17	53.30	0.00	23.47	0.04	0.00	0.00	8.75	8.05	0.73	96.32	2.56	0.01	0.00	7.72	4.00	0.00	0.00	0.00	0.00	0.00	1.36	2.26	0.14	15.47	38
			18	53.87	0.01	23.29	0.04	0.00	0.03	8.62	8.08	0.74	96.67	2.58	0.00	0.00	7.76	3.95	0.00	0.00	0.00	0.00	0.00	1.33	2.26	0.14	15.45	37
PIES-5F1	amphibole	1	10	48.73	0.00	27.88	0.10	0.00	0.00	17.11	4.22	0.07	98.88	0.82	0.19	0.01	6.91	4.65	0.00	0.01	0.00	0.00	0.00	2.60	1.16	0.01	15.34	69
			11	48.38	0.00	28.21	0.06	0.03	0.04	17.24	3.78	0.32	98.73	0.83	0.04	0.00	6.87	4.71	0.00	0.01	0.00	0.00	0.01	2.62	1.04	0.06	15.32	72
			13	49.36	0.00	26.93	0.37	0.75	0.00	15.56	4.43	0.12	98.24	0.92	0.00	0.00	7.02	4.51	0.00	0.04	0.00	0.00	0.16	2.37	1.22	0.02	15.34	66

Table 5. Chemical composition (weight %) of selected phlogopite and olivine, obtained by electron microprobe (EMP)and scanning electronic microscopy (SEM), and its cationic distribution.

Phlogopite	ITA-68A1 (EMP)						PIES-5F1 (EMP)			PIES-5A1 (SEM)		ESC... (EMP)				Esc+++ (EMP)	
Zone	hornblende granofels			contact between skarn and dike			amphibolite			carbonate + olivine	diopside + hornblende	Contact between carbonate + tremolite and diopside zones		vein		Contact between diopside and scapolite + diopside zones	
Location	1w			4w			2z			1k	5k	3a		5a		2b	
Spot	7	8	9	1	2	3	4	5	6	15	11	1	2	1	2	1	2
SiO_2	40.05	40.06	40.56	39.59	39.63	40.12	40.97	41.02	40.09	43.91	41.56	41.98	41.56	42.25	42.54	41.17	40.89
TiO_2	0.81	0.68	0.81	0.68	0.70	0.74	1.69	1.40	1.40			0.20	0.08	0.33	0.20	0.21	0.18
Al_2O_3	17.35	17.99	18.21	17.00	16.66	16.94	16.97	17.26	16.68	13.12	16.26	12.66	12.83	14.37	13.96	15.26	15.00
FeOt*	3.74	3.88	3.85	4.20	4.58	4.28	6.95	7.43	6.78	4.48	9.12	1.03	1.07	1.52	1.29	2.42	2.38
MgO	22.76	23.03	23.27	23.25	23.29	23.68	20.01	20.40	20.29	26.24	21.22	27.19	27.04	26.48	26.45	25.31	24.88
MnO	0.04	0.04	0.00	0.00	0.05	0.00	0.00	0.02	0.03			0.00	0.00	0.00	0.00	0.03	0.04
CaO	0.04	0.08	0.03	0.01	0.02	0.02	0.07	0.04	0.07			0.14	0.01	0.06	0.02	0.02	0.01
Na_2O	0.41	0.47	0.56	0.32	0.29	0.30	0.58	0.60	0.59			0.06	0.08	0.08	0.14	0.13	0.07
K_2O	9.12	8.63	9.11	9.42	9.41	9.52	8.11	8.33	8.16	12.24	11.83	10.27	10.34	10.30	10.32	9.92	9.62
F	0.45	0.80	0.60	0.84	1.19	1.00	0.53	0.70	0.84			2.17	2.04	1.59	1.74	1.52	1.83
Cl	0.08	0.08	0.07	0.10	0.14	0.12	0.05	0.02	0.04			0.06	0.05	0.03	0.03	0.06	0.06
Total	94.67	95.39	96.84	95.06	95.45	96.27	95.71	96.96	94.64	99.99	99.99	94.83	94.23	96.38	95.99	95.38	94.18
Si	5.67	5.63	5.62	5.63	5.64	5.64	5.78	5.74	5.74	5.97	5.76	5.97	5.94	5.89	5.95	5.81	5.85
AlIV	2.33	2.37	2.38	2.37	2.36	2.36	2.22	2.26	2.26	2.03	2.24	2.03	2.06	2.11	2.05	2.19	2.16
AlVI	0.57	0.60	0.59	0.47	0.43	0.44	0.60	0.58	0.56	0.08	0.42	0.09	0.11	0.25	0.25	0.35	0.37
Ti	0.09	0.07	0.08	0.07	0.07	0.08	0.18	0.15	0.15	0.00	0.00	0.02	0.01	0.04	0.02	0.02	0.02
Fe^{2+}	0.44	0.46	0.45	0.50	0.55	0.50	0.82	0.87	0.81	0.51	1.06	0.12	0.13	0.18	0.15	0.29	0.29
Mn	0.01	0.00	0.00	0.00	0.01	0.00	0.00	0.00	0.00	0.00	0.00	0.00	0.00	0.00	0.00	0.00	0.01
Mg	4.81	4.82	4.81	4.93	4.94	4.96	4.21	4.26	4.33	5.32	4.39	5.76	5.77	5.50	5.51	5.33	5.30
Ca	0.01	0.01	0.01	0.00	0.00	0.00	0.01	0.01	0.01	0.00	0.00	0.02	0.00	0.01	0.00	0.00	0.00
Na	0.11	0.13	0.15	0.09	0.08	0.08	0.16	0.16	0.16	0.00	0.00	0.02	0.02	0.02	0.04	0.04	0.02
K	1.65	1.55	1.61	1.71	1.71	1.71	1.46	1.49	1.49	2.13	2.09	1.86	1.89	1.83	1.84	1.79	1.76
Cations	15.67	15.65	15.69	15.77	15.78	15.77	15.44	15.51	15.52	16.03	15.95	15.89	15.92	15.82	15.82	15.81	15.76
CF	0.41	0.71	0.53	0.76	1.07	0.89	0.47	0.62	0.76	0.00	0.00	1.95	1.85	1.40	1.54	1.35	1.65
CCl	0.04	0.04	0.03	0.05	0.07	0.06	0.02	0.01	0.02	0.00	0.00	0.03	0.02	0.02	0.02	0.03	0.03
Annite	0.08	0.09	0.08	0.09	0.10	0.09	0.16	0.17	0.16	0.09	0.19	0.02	0.02	0.03	0.03	0.05	0.05
Phlogopite	0.92	0.91	0.92	0.91	0.90	0.91	0.84	0.83	0.84	0.91	0.81	0.98	0.98	0.97	0.97	0.95	0.95

Olivine	ITA-68A1 (EMP)	PIES-2F1 (SEM)				PIES-5A1 (SEM)		ESC... (EMP)	
Zone	carbonate + olivine							carbonate + tremolite	
Location	2w	4y				1k	3k	1a	
Spot	10	11	26	31	33	11	13	1	2
SiO_2	41.56	37.61	2.62	31.99	37.54	38.50	39.11	42.09	42.44
TiO_2	0.03							0.00	0.08
Al_2O_3	0.00	0.43			0.57	0.48	0.32	0.05	0.00
FeOt*	12.31	18.67	5.41	15.64	21.14	14.90	13.74	1.40	1.55
MgO	47.30	42.88	35.37	39.37	39.85	45.68	46.49	55.74	54.73
MnO	0.08	0.41						0.05	0.09
CaO	0.00		56.60	13.01	0.55			0.03	0.02
Na_2O	0.01				0.35	0.45	0.34	0.00	0.03
Total	101.42	100.00	100.00	100.01	100.00	100.01	100.00	99.45	98.95
Si	1.01	0.97	0.09	0.86	0.97	0.97	0.98	1.00	1.01
Al	0.00	0.01	0.00	0.00	0.02	0.01	0.01	0.00	0.00
Ti	0.00	0.00	0.00	0.00	0.00	0.00	0.00	0.00	0.00
Fe^{2+}	0.25	0.40	0.15	0.35	0.46	0.31	0.29	0.03	0.03
Mn	0.00	0.01	0.00	0.00	0.00	0.00	0.00	0.00	0.00
Mg	1.72	1.64	1.71	1.57	1.54	1.72	1.73	1.97	1.94
Ca	0.00	0.00	1.97	0.37	0.02	0.00	0.00	0.00	0.00
Na	0.00	0.00	0.00	0.00	0.02	0.02	0.02	0.00	0.00
Cations	2.99	3.03	3.92	3.15	3.03	3.04	3.02	3.00	2.99
Fa	13	20	8	18	23	15	14	1	2
Fo	87	80	92	82	77	85	86	99	98

Table 6. Chemical composition (weight %) of selected spinel and chlorite, obtained by electron microprobe (EMP) and scanning electronic microscopy (SEM), and its cationic distribution.

Spinel	ITA-68A1						Chlorite	ITA-68A1			ITA-68A (SEM)			
Zone	carbonate + olivine						Banda	carbonate + olivine			carbonate + olivine			
Location	1w			2w			Location	2w			4x		2x	
Spot	1	3	4	1	2	3	Spot	4	5	6	11	16	12	18
SiO_2	0.01	0.03	0.06	0.07	0.03	0.03	SiO_2	28.21	29.56	29.29	35.40	37.42	35.28	35.52
TiO_2	0.05	0.02	0.09	0.04	0.01	0.00	TiO_2	0.03	0.10	0.05				
Al_2O_3	68.55	68.11	67.88	67.94	68.09	68.41	Al_2O_3	21.91	22.78	22.60	22.23	21.58	22.50	22.52
FeOt*	13.88	14.46	13.64	13.15	13.70	13.80	FeOt*	4.38	4.47	4.12	5.96	5.50	6.70	6.47
MgO	17.58	17.67	17.50	18.43	18.88	18.50	MgO	28.71	30.03	29.51	35.84	35.51	35.53	35.38
MnO	0.05	0.06	0.03	0.11	0.04	0.11	MnO	0.00	0.04	0.04				0.06
CaO	0.00	0.01	0.04	0.03	0.00	0.05	CaO	0.11	0.05	0.05	0.07			
Na_2O	0.04	0.00	0.00	0.03	0.02	0.03	Na_2O	0.08	0.03	0.06	0.50			
K_2O	0.02	0.01	0.01	0.02	0.01	0.03	K_2O	0.04	0.02	0.03				0.05
Total	100.18	100.40	99.37	99.85	100.82	101.08	Total	83.531	87.195	85.942	100	100.01	100.01	100
Al	16.23	16.14	16.21	16.11	16.02	16.08	Si	3.98	3.99	4.01	4.19	4.39	4.18	4.20
Fe^{2+}	2.33	2.43	2.31	2.21	2.29	2.30	AlIV	3.64	3.62	3.64	3.10	2.98	3.14	3.14
Mg	5.27	5.30	5.29	5.53	5.62	5.51	Sum T	7.61	7.61	7.65	7.28	7.37	7.31	7.34
Cations	23.87	23.90	23.85	23.91	23.96	23.94	AlVI	0.00	0.00	0.00	0.00	0.00	0.00	0.00
Fe/(Fe+Mg)	30.70	31.45	30.42	28.59	28.93	29.50	Ti	0.00	0.01	0.01	0.00	0.00	0.00	0.00
							Fe^{2+}	0.52	0.50	0.47	0.59	0.54	0.66	0.64
							Mn	0.00	0.00	0.00	0.00	0.00	0.00	0.01
							Mg	6.03	6.04	6.02	6.32	6.21	6.27	6.24
							Ca	0.02	0.01	0.01	0.01	0.00	0.00	0.00
							Na	0.02	0.01	0.02	0.12	0.00	0.00	0.00
							K	0.01	0.00	0.01	0.00	0.00	0.00	0.01
							Cations	14.21	14.19	14.17	14.32	14.12	14.25	14.23
							Fe/(Fe+Mg)	0.08	0.08	0.07	0.09	0.08	0.10	0.09
							Mg/(Fe+Mg)	0.92	0.92	0.93	0.91	0.92	0.90	0.91

Table 7. Chemical composition (weight %) of selected feldspar, obtained by EMP, and its cationic distribution.

Feldspar	Zone	Location	Spot	SiO_2	TiO_2	Al_2O_3	FeOt*	MgO	MnO	CaO	Na_2O	K_2O	Total	Si	Al	Ti	Fe^{2+}	Mn	Mg	Ca	Na	K	Cations	Ab	An	Or
PIES-5F1	amphibolite	1z	12	46.18	0.00	36.10	0.03	0.00	0.01	19.53	0.73	0.01	102.72	8.31	7.65	0.00	0.01	0.00	0.00	3.76	0.25	0.00	19.98	6.30	93.60	0.00
			7	46.86	0.04	36.21	0.07	0.04	0.01	18.94	0.99	0.06	103.22	8.37	7.61	0.01	0.01	0.00	0.01	3.62	0.34	0.01	19.99	8.60	91.00	0.40
			8	44.37	1.22	14.23	7.72	15.13	0.09	12.84	1.96	1.20	99.15	8.81	3.33	0.18	1.28	0.02	4.48	2.73	0.76	0.30	21.88	20.00	72.10	8.00
			9	46.37	0.01	36.26	0.09	0.00	0.07	19.20	0.76	0.02	102.78	8.32	7.66	0.00	0.01	0.01	0.00	3.69	0.27	0.00	19.97	6.70	93.20	0.10
		2z	1	45.47	0.00	36.05	0.04	0.00	0.03	19.61	0.65	0.01	101.85	8.25	7.70	0.00	0.01	0.00	0.00	3.81	0.23	0.00	20.00	5.60	94.30	0.10
			2	46.39	0.09	36.01	0.08	0.00	0.00	19.56	0.81	0.01	102.99	8.32	7.61	0.01	0.01	0.00	0.00	3.76	0.28	0.00	19.99	6.90	93.00	0.00
			3	45.51	0.00	36.53	0.01	0.00	0.03	19.96	0.51	0.01	102.61	8.20	7.75	0.00	0.00	0.00	0.00	3.86	0.18	0.00	20.00	4.50	95.50	0.10
CAS29Pb	granite	1c	7	65.35	0.08	21.63	0.04	0.01	0.02	2.93	9.22	0.12	99.47	11.54	4.50	0.01	0.01	0.00	0.00	0.55	3.15	0.03	19.79	84.40	14.80	0.70
			8	65.93	0.03	18.42	0.05	0.01	0.00	0.02	0.42	16.18	101.15	12.04	3.96	0.00	0.01	0.00	0.00	0.00	0.15	3.77	19.93	3.80	0.10	96.10
Esc+++		4b	7	64.38	0.00	18.92	0.07	0.01	0.02	0.01	0.59	16.11	100.12	11.90	4.12	0.00	0.01	0.00	0.00	0.00	0.21	3.80	20.04	5.20	0.00	94.70
			8	64.54	0.00	18.99	0.01	0.01	0.00	0.02	0.76	15.59	99.97	11.91	4.13	0.00	0.00	0.00	0.00	0.00	0.27	3.67	19.99	6.90	0.10	93.00
			9	64.44	0.00	18.86	0.06	0.00	0.06	0.01	0.51	15.81	99.79	11.93	4.11	0.00	0.01	0.01	0.00	0.00	0.18	3.73	19.97	4.70	0.00	95.30
PIES-1B1		1d	23	62.99	0.01	23.05	0.16	0.01	0.05	3.92	8.86	0.16	99.24	11.21	4.83	0.00	0.02	0.01	0.00	0.75	3.06	0.04	19.92	79.60	19.40	1.00
			24	62.00	0.00	22.31	0.02	0.00	0.02	3.48	8.60	0.12	96.65	11.30	4.79	0.00	0.00	0.00	0.00	0.68	3.04	0.03	19.84	81.10	18.20	0.70
		5d	5	63.94	0.00	18.40	0.00	0.00	0.00	0.04	0.75	15.77	98.98	11.95	4.05	0.00	0.00	0.00	0.00	0.01	0.27	3.76	20.04	6.70	0.20	93.10
			6	62.73	0.01	18.52	0.03	0.01	0.00	0.03	0.62	14.68	96.77	11.93	4.15	0.00	0.00	0.00	0.00	0.01	0.23	3.56	19.88	6.00	0.20	93.80
			7	59.85	0.05	18.12	2.05	1.89	0.03	0.02	0.53	14.18	96.75	11.54	4.12	0.01	0.33	0.00	0.54	0.00	0.20	3.49	20.23	5.40	0.10	94.50
			8	61.90	0.04	22.75	0.09	0.02	0.02	2.61	8.57	0.05	96.05	11.30	4.89	0.01	0.01	0.00	0.01	0.51	3.03	0.01	19.77	85.30	14.30	0.30

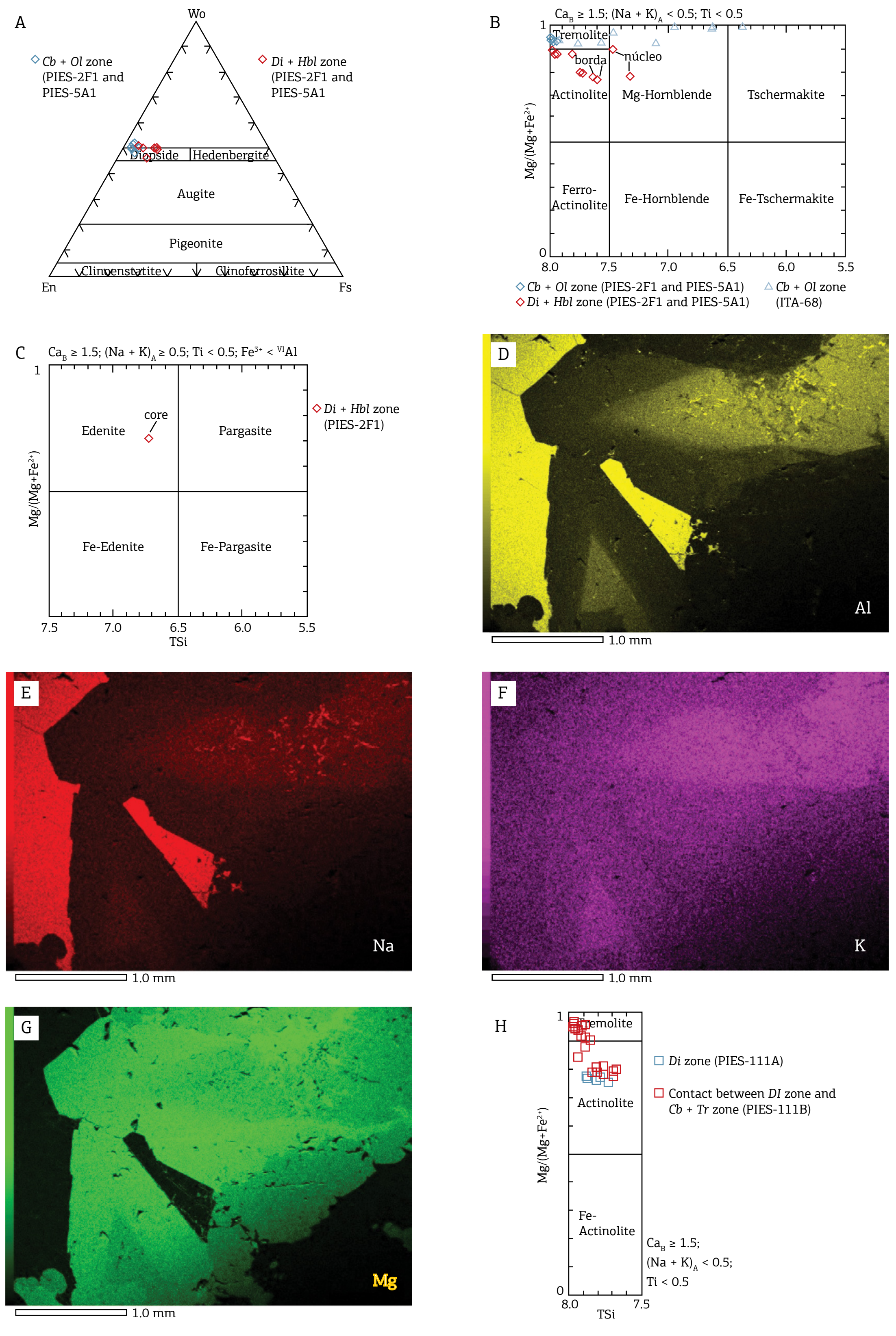

SEM: scanning electronicmicroscopy.

Figure 8.(A, B andC) Pyroxene and amphibole classification of skarns associated with metamafic dykes; (D, E, F and G) amphibole compositional maps obtained by SEM of skarns associated with metamafic dykes; (H) amphibole classification of skarns associated with felsic dykes.

In the *scapolite* + *diopside* zone belonging to the skarn associated with the alkali-feldspar granite, the composition of scapolite varies from more calcic when closer to the marble (Me = 60 – 65), to more sodic closer to the granite (Me = 27 – 45) (Table 4). Compositional zoning occurs with increase of Ca toward the border.

Olivine

The composition of olivine is essentially Mg-rich (Fo_{77} – Fo_{99}), and it was classified as forsterite and chrysolite (Fig. 9A). Forsterite was found mainly in the skarn adjacent to the granitic dyke, while chrysolite, in which the Fe-content is higher (Fa_{13} – Fa_{23}), was found in the skarn associated with the metamafic dyke (Table 5).

Phlogopite

The type of mica that occurs in the skarns and in the metamafic dykes is phlogopite (81 to 98% of the phlogopite component) (Table 5). The diagram of Figure 9B shows that the phlogopite found in *carbonate* + *olivine* zone in the skarn associated with the metamafic dyke has higher content of Mg and lower content of Fe and Al when compared to that one found in the *diopside* + *hornblende* zone, which is closer to the dyke. More Fe-rich compositions are observed in the skarns associated with the mafic dykes.

In the skarns associated with the felsic dykes, the phlogopite-rich zones (Fig. 6) that occur at the boundaries between the zones present a small compositional variation with increase of Mg toward the marble. At the contact between the zones *carbonate* + *tremolite* and *diopside*, phlogopite has 2% of annite component, while at the contact between zones *diopside* and *scapolite* + *diopside* the content of annite is 5% (Table 5). The phlogopite at the border of the carbonate veins found in the *diopside* zone has 3% of annite. The content of Al is a little lower at the contact of zones *carbonate* + *tremolite* and *diopside* (Al_{IV} = 2.03 – 2.06), than of zones *diopside* and *scapolite* + *diopside* (Al_{IV} = 2.13 – 2.19).

Spinel

The spinel from the hornblende granofels and related skarn is Al-rich and belongs to the solid solution in which the end-member are spinel *sensu stricto* and hercynite. Spinel is classified as pleonaste, in which the hercynite component varies between 29 and 31% (Table 6).

Chlorite

Chlorite is essentially Mg-rich with X_{Mg} = 0.92 – 0.93 (Table 6). This chlorite occurs as replacement of pleonaste in the skarn associated with the hornblende granofels.

Feldspar

The feldspar from the amphibolite dykes was classified as anorthite (An_{91-96}) and bytownite (An_{72}). In the alkali-feldspar granite, the plagioclase was classified as oligoclase (An_{14-19}), and the alkali-feldspar as orthoclase (Or_{93-96}) (Table 7).

Geochronology

The alkali-feldspar granite was selected for U-Pb geochronology analyses because of its lack of metamorphic overprinting, so that skarns related to it were essentially generated by the late to post-tectonic intrusion.

The selected zircon grains from the sample PIES-1-C are well-formed, elongated, bipyramidal-prismatic and colorless to yellowish, often transparent. The length/width ratio varies from 2:1 to 4:1. The zircons may be fractured and broken and the cathodoluminescence images display a magmatic

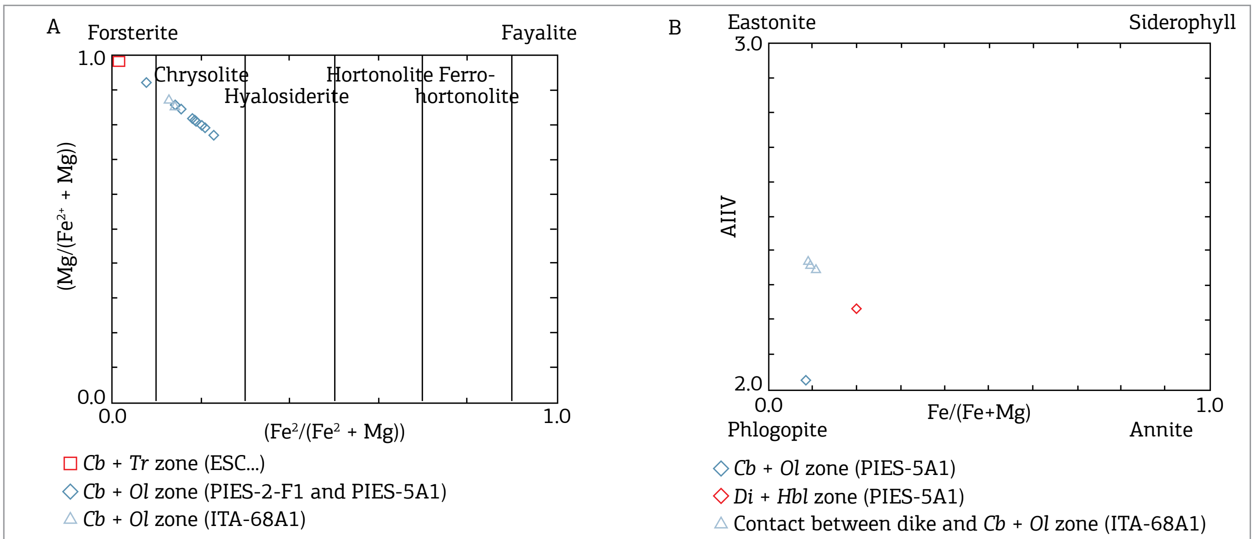

Figure 9. Classification of olivine (A) and biotite (B) of skarn associated with metamafic dykes.

oscillatory zoning (Fig. 10). The analyses were performed on 60 spots of 51 zircon grains. The Th/U ratio is typically magmatic, higher than 0.2 (Table 8).

Eight analyses with discordance values less than 4%, individual ratios errors less than 7% and common Pb less than 100 counts per second (c/s) were selected and plotted on Figure 11A. These eight most concordant analyses provided a discordant age of 541 ± 15 Ma for the superior intercept, which is confirmed by three concordant grains that show a concordant age of 541 ± 9 Ma (Fig. 11B), being the best estimative for the magmatic crystallization age. This age is related to the late- to post-collisional stage (545–530 Ma) of the Araçuaí orogen (Pedrosa-Soares & Wiedemann-Leonardos 2000, Pedrosa-Soares *et al.* 2001, 2007, 2011; Silva *et al.* 2005).

Since the skarns associated with the granitoids were formed concomitantly to the crystallization of these rocks, the obtained age of 541 ± 9 Ma can evidence the timing of skarnitization.

DISCUSSION

The skarns in the study area can be divided into two main types: skarns related to metamafic dykes, and skarns related to felsic dykes.

The metamafic dykes are represented by amphibolite and hornblende granofels. They were intensely deformed, folded, disrupted and metamorphosed. The presence of pargasite

Figure 10. Cathodoluminescence images of zircon grains from the alkali-feldspar granite, sample PIES-1C. Spots used for the Concordia Age (**).

Table 8. LA-ICP-MS zircon U-Pb dating results from 60 spot analyses.

Spot number-Grain number	Ratios							Age (Ma)						%	^{204}Pbc/s	^{232}Th/^{238}U
	^{207}Pb*/^{235}U	±	^{206}Pb*/^{238}U	±	Rho 1	^{207}Pb*/^{206}Pb*	±	^{206}Pb/^{238}U	±	^{207}Pb/^{235}U	±	^{207}Pb/^{206}Pb	±	Disc.		
018-zircon 1	0.655244	0.0054	0.076960	0.0005	0.74	0.061750	0.0007	478	3	512	3	665	25	7	0	0.28
019-zircon 1**	0.683413	0.0086	0.084540	0.0006	0.59	0.058630	0.0009	523	4	529	5	553	33	1	94	0.39
020-zircon 2**	0.653281	0.0143	0.080620	0.0008	0.48	0.058770	0.0014	500	5	510	9	559	52	2	11	0.63
021-zircon 3	0.625588	0.0085	0.075414	0.0006	0.58	0.060163	0.0010	469	4	493	5	609	33	5	0	0.59
022-zircon 4	0.599248	0.0057	0.072567	0.0004	0.64	0.059892	0.0008	452	3	477	3	600	27	6	86	0.41
025-zircon 5	0.800646	0.0063	0.077208	0.0005	0.78	0.075210	0.0009	479	3	597	3	1074	22	25	384	0.12
026-zircon 6	0.786288	0.0052	0.073770	0.0004	0.89	0.077304	0.0008	459	3	589	3	1129	20	28	611	0.31
027-zircon 7	0.651194	0.0049	0.076410	0.0005	0.79	0.061810	0.0007	475	3	509	3	668	24	7	0	0.33
031-zircon 8	0.679138	0.0058	0.079859	0.0005	0.74	0.061678	0.0007	495	3	526	3	663	25	6	142	0.58
033-zircon 9	0.856204	0.0076	0.085440	0.0006	0.73	0.072680	0.0009	529	3	628	4	1005	25	19	7	0.51
034-zircon 10**	0.641461	0.0100	0.078520	0.0007	0.54	0.059250	0.0011	487	4	503	6	576	39	3	97	0.62
035-zircon 11	0.570559	0.0054	0.073285	0.0005	0.65	0.056466	0.0007	456	3	458	3	471	26	1	132	0.38
037-zircon 12	0.698422	0.0052	0.082620	0.0005	0.77	0.061310	0.0007	512	3	538	3	650	24	5	93	0.07
038-zircon 12	0.815333	0.0065	0.072821	0.0005	0.82	0.081204	0.0009	453	3	605	3	1226	21	34	367	0.31
039-zircon 13	0.547491	0.0054	0.073907	0.0005	0.66	0.053727	0.0007	460	3	443	3	360	26	-4	159	0.10
040-zircon 14**	0.633898	0.0052	0.077799	0.0005	0.78	0.059094	0.0007	483	3	499	3	571	25	3	43	0.31
044-zircon 15	0.185818	0.0179	0.048929	0.0009	0.20	0.027544	0.0018	308	6	173	11	1430	64	-44	63	0.77
045-zircon 16	0.879994	0.0075	0.082962	0.0005	0.76	0.076931	0.0009	514	3	641	4	1119	23	25	232	0.55
046-zircon 16	0.898050	0.0074	0.071005	0.0004	0.75	0.091729	0.0011	442	3	651	4	1462	21	47	574	0.39
047-zircon 17	0.828199	0.0091	0.074539	0.0005	0.65	0.080585	0.0011	463	3	613	4	1211	24	32	324	0.40
049-zircon 18	0.918877	0.0082	0.080804	0.0005	0.72	0.082475	0.0010	501	3	662	4	1257	23	32	209	0.55
050-zircon 19	0.802728	0.0058	0.077580	0.0004	0.76	0.075045	0.0009	482	3	598	3	1070	22	24	488	0.21
051-zircon 20	0.736747	0.0118	0.090260	0.0008	0.52	0.059200	0.0011	557	4	561	7	574	40	1	26	0.67
052-zircon 21	1.019920	0.0079	0.074847	0.0005	0.87	0.098830	0.0011	465	3	714	4	1602	19	53	1080	0.21
058-zircon 22	1.104158	0.0105	0.109844	0.0008	0.74	0.072905	0.0009	672	4	755	5	1011	26	12	86	0.33
059-zircon 23	1.111080	0.0188	0.071174	0.0008	0.63	0.113220	0.0019	443	4	759	8	1852	28	71	184	0.85
060-zircon 24	0.769804	0.0062	0.077524	0.0005	0.75	0.072018	0.0008	481	3	580	4	986	23	20	281	0.15
061-zircon 25	0.734023	0.0064	0.078476	0.0005	0.76	0.067838	0.0008	487	3	559	4	864	24	15	263	0.31
062-zircon 26	0.704284	0.0065	0.077483	0.0005	0.67	0.065923	0.0008	481	3	541	4	804	26	13	105	0.86
063-zircon 27	0.851474	0.0066	0.085830	0.0005	0.78	0.071950	0.0008	531	3	625	4	985	23	18	63	0.46
064-zircon 28	0.639260	0.0124	0.076394	0.0007	0.50	0.060690	0.0012	475	4	502	7	628	36	6	159	0.79
065-zircon 29	0.757950	0.0061	0.076911	0.0005	0.76	0.071474	0.0008	478	3	573	3	971	23	20	319	0.40
066-zircon 30	1.114573	0.0101	0.077341	0.0005	0.77	0.104519	0.0013	480	3	760	4	1706	21	58	705	0.18
070-zircon 31	0.825493	0.0065	0.092489	0.0006	0.81	0.064733	0.0007	570	3	611	3	766	23	7	223	0.35
071-zircon 32	1.050469	0.0090	0.082520	0.0006	0.78	0.092326	0.0011	511	3	729	4	1474	22	43	147	0.36
072-zircon 32	0.674414	0.0052	0.048223	0.0003	0.87	0.101431	0.0011	304	2	523	3	1650	19	72	2193	0.34
073-zircon 33**(C.A.)	0.687889	0.0067	0.086208	0.0006	0.66	0.057872	0.0008	533	3	532	4	525	28	0	28	0.46
074-zircon 34	0.919178	0.0083	0.069334	0.0005	0.73	0.096150	0.0012	432	3	662	4	1551	21	53	944	0.20
075-zircon 35	0.722617	0.0064	0.085790	0.0005	0.71	0.061090	0.0008	531	3	552	4	642	26	4	70	0.73
076-zircon 35	0.773820	0.0067	0.083827	0.0006	0.78	0.066950	0.0008	519	3	582	4	836	24	12	287	0.60
077-zircon 36	0.746129	0.0058	0.082018	0.0005	0.83	0.065978	0.0007	508	3	566	3	806	23	11	150	0.28
079-zircon 37	0.742309	0.0077	0.090880	0.0006	0.65	0.059240	0.0008	561	4	564	4	576	29	1	20	0.46
080-zircon 37	0.704532	0.0063	0.084051	0.0006	0.76	0.060793	0.0007	520	3	541	4	632	25	4	121	0.38
081-zircon 38	0.906176	0.0126	0.086980	0.0007	0.57	0.075560	0.0013	538	4	655	7	1083	34	22	13	0.70
082-zircon 39	1.217291	0.0155	0.106910	0.0008	0.61	0.082580	0.0013	655	5	809	7	1259	30	23	39	0.63
083-zircon 40	0.714808	0.0093	0.085030	0.0006	0.56	0.060970	0.0010	526	4	548	5	638	34	4	5	0.89
084-zircon 40**(C.A.)	0.716765	0.0086	0.088560	0.0006	0.59	0.058700	0.0009	547	4	549	5	556	32	0	0	0.58
088-zircon 41	0.859622	0.0071	0.093732	0.0006	0.73	0.066515	0.0008	578	3	630	4	823	24	9	283	0.32
089-zircon 42	0.926748	0.0095	0.083610	0.0006	0.67	0.080390	0.0011	518	3	666	5	1207	26	29	33	0.90
090-zircon 42	0.792324	0.0068	0.081622	0.0005	0.73	0.070404	0.0008	506	3	592	4	940	24	17	204	0.86
091-zircon 43	0.660713	0.0072	0.084536	0.0006	0.65	0.056685	0.0008	523	4	515	4	479	28	-2	112	0.45
092-zircon 43**	0.662095	0.0054	0.081680	0.0005	0.77	0.058790	0.0007	506	3	516	3	559	25	2	44	0.28
093-zircon 44**(C.A.)	0.718307	0.0125	0.088690	0.0008	0.53	0.058740	0.0012	548	5	550	7	557	42	0	60	0.49
095-zircon 45	1.080292	0.0150	0.099190	0.0008	0.58	0.078990	0.0013	610	5	744	7	1172	33	22	48	0.55
096-zircon 46	0.687537	0.0059	0.076867	0.0005	0.73	0.064872	0.0008	477	3	531	4	770	25	11	139	0.25
097-zircon 47	0.820311	0.0089	0.083306	0.0006	0.66	0.071417	0.0010	516	4	608	5	969	26	18	165	0.60
098-zircon 48	0.628811	0.0072	0.080802	0.0006	0.61	0.056441	0.0008	501	3	495	4	470	30	-1	62	0.81
100-zircon 49	1.261203	0.0147	0.087860	0.0007	0.64	0.104110	0.0015	543	4	828	7	1699	27	53	228	0.42
101-zircon 50	1.108266	0.0139	0.115620	0.0009	0.59	0.069520	0.0011	705	5	757	7	914	31	7	143	0.38
102-zircon 51	0.746142	0.0085	0.091180	0.0007	0.66	0.059350	0.0008	563	4	566	5	580	30	1	31	0.37

**Analyses used for the Discordia Diagram. (C.A.) Analyses used for the Concordia Age.
Discordant (Disc.); Counts per second (c/s).
1. Sample and standard are corrected after Pb and Hg blanks.
2. ^{207}Pb/^{206}Pb and ^{206}Pb/^{238}U are corrected after common Pb presence. Common Pb assuming ^{206}Pb/^{238}U and ^{207}Pb/^{235}U concordant age.
3. ^{235}U = 1/137.88*Utotal
4. Standard M127
5. Th/U = ^{232}Th/^{238}U * 0.992743
6. All errors in the table are calculated 1 sigma (% for isotope ratios, absolute for ages).

and spinel indicates that they were metamorphosed under P-T granulite facies conditions.

Associated with the metamafic dykes, two main skarn zones were identified from marble towards the dyke (Fig. 4): *carbonate + olivine* and *diopside + hornblende*. These skarn zones are probably generated at the expenses of the marble due to the metasomatic infiltration of elements originated from the intrusion and, thus, are exoskarns. Mesquita (2016) discusses that the substantial decrease of elements of low mobility such as Al and Ti from the dyke to the adjacent skarn is an evidence for it to be an exoskarn. However, it is also possible that the metamorphic event that affected the mafic dykes, skarns and marbles may have promoted an additional exchange of elements between the rock types. In other words, the skarns related to the metamafic dykes were probably generated by metasomatic processes at the time of the intrusion, but they were recrystallized during the high grade regional metamorphic event, as discussed by Jordt-Evangelista and Viana (2000).

Mineral chemistry data show that in all skarns diopside, amphibole and phlogopite are more enriched in Mg in the zones closer to the marble. It suggests a contribution of this element from reactions involving dolomite. In the skarns related to the amphibolite (Fig. 4), the higher content of Fe in the amphibole from the *diopside + hornblende* zone suggests contribution of this element from the dyke, rich in mafic minerals.

Regarding olivine, it was found that the contribution of Fe from the metamafic dyke provides the formation of less magnesian compositions (chrysolite) than in the olivine related to the granitic dykes (forsterite). Moreover, its occurrence in the skarn portions closer to the marble is due to the lower content of Si in this rock. The migration of this element is hampered by the distance since its supply is derived from the dykes that generate minerals increasingly more depleted in Si towards the marble.

Phlogopite is also more enriched in Fe in the skarns related to the metamafic dykes (Phl_{81-91}) than in the skarns related to the felsic dykes (Phl_{95-98}), which supports the idea of contribution of Fe from the metamafic dyke.

The felsic dykes are composed of alkali-feldspar granite, monzogranite or syenogranite. The first two granitoids generally do not show evidence of deformation (or show incipient deformation features as undulatory extinction on quartz grains) and metamorphism, while the last one is weakly foliated, but still preserves relicts of the igneous minerals and texture.

In the skarns related to the felsic dykes three well-defined mineralogical zones were identified from marble towards the granite (Fig. 6): *carbonate + tremolite*; *diopside*; and *scapolite + diopside*. Two of these zones (*carbonate + tremolite* and *diopside*) were identified as having the marble as protolith, so called as exoskarns. The other zone (*scapolite + diopside*) is an endoskarn formed at the expenses of the alkali-feldspar granite. This interpretation was made possible by field-based observations that show a gradual transition between the granite and the endoskarn and an abrupt contact between the endoskarn and the exoskarn. The occurrence of zircon in the *scapolite + diopside* zone is also an evidence that it is in fact an endoskarn since this mineral is not found in the studied marbles. Other arguments concerning the classification of the studied zones as endo or exoskarns are based on their chemical composition in terms of major, trace and REE elements as discussed by Mesquita (2016), who considers that the abrupt decrease of Al and Ti, as well as of the

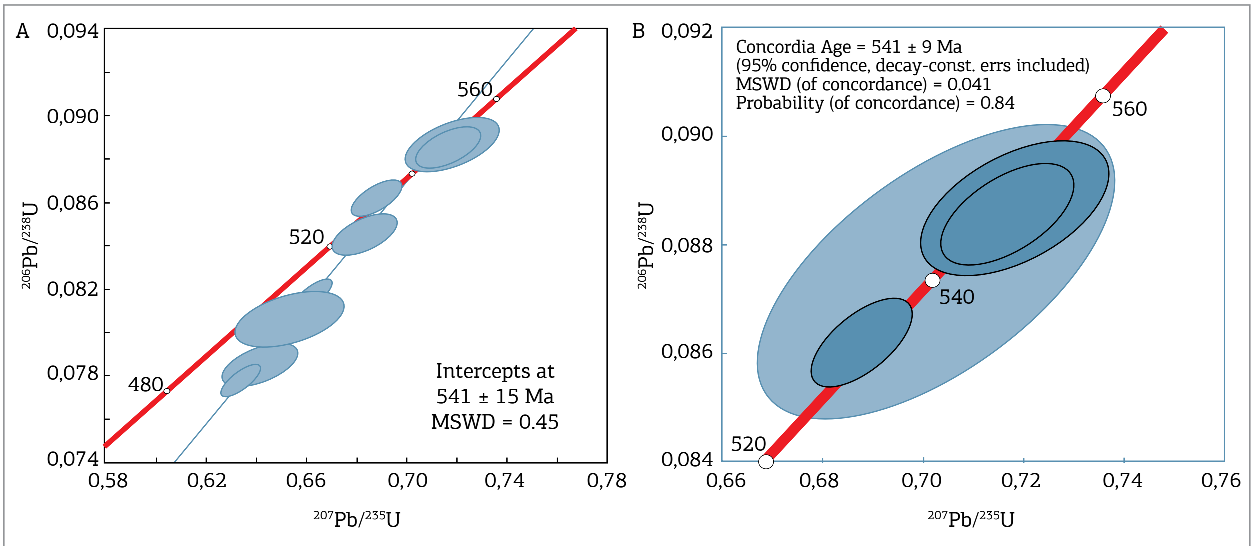

Figure 11. U-Pb diagrams of LA-ICP-MS analyses from zircons of the alkali-feldspar granite, sample PIES-1C. (A) Discordia diagram; (B) Concordia diagram.

most of trace elements from the *scapolite + diopside* zone to the *diopside* zone, suggests that the first zone is an endoskarn and the second one is an exoskarn.

Concerning mineral chemistry data in the skarns related to the felsic dykes, the migration of Si and aqueous fluids achieved larger distances as shown by the larger skarn zones and by the occurrence of amphiboles such as actinolite and tremolite closer to the marble (Fig. 6), since amphiboles require the presence of H_2O and a higher Si-content than olivine.

The formation of skarns is promoted by the chemical potential gradients between marble and dykes. Since there is substantial contrast in the chemical compositions of granite and marble in comparison with amphibolite and marble, the generation of skarns associated with granitoids is more effective. The migration of elements is also facilitated by fluids which are more abundant in felsic magmas than in mafic magmas.

Another element that had some mobility was Al derived from the dykes, responsible for the generation of phlogopite-rich seams at the contact between the zones (Fig. 6). The smaller quantity of Al in the phlogopite closer to the marble reveals the decrease of mobility.

Regarding the scapolite, there are an increase of the calcic component (meionite) and a decrease of the sodic component (marialite) from granite towards the marble, indicating an input of calcium from the marble while the granite would be the source of the sodium. The compositional zoning detected in some scapolites that show increase of the meionite-content towards the border indicates that the supply of calcium was higher than the supply of sodium during the formation of the skarn. In the amphibolites, scapolite occurs as a replacement of plagioclase. Since this plagioclase is rich in anorthite component, more calcic scapolites were formed with up to 72% of the meionite component. Probably, the anion CO_3^{2-} was derived from the marble.

Medeiros Junior (2016) obtained temperatures of 690 to 790ºC for the metamorphism of the marbles and related calc-silicate rocks from the Paraíba do Sul Complex in the study region. Similar metamorphic conditions are corroborated by the occurrence of pargasite and spinel and by the deformation features in the metamafic dykes and related skarns. Therefore, the skarns related to the metamafic dykes were probably recrystallized in the same event that metamorphosed the Paraíba do Sul rocks during the syn-collisional stage of the Araçuaí orogen, between 580 and 560 Ma (Pedrosa-Soares & Wiedemann-Leonardos 2000, Pedrosa-Soares *et al.* 2001, 2007, 2011; Silva *et al.* 2005). Retrometamorphic processes provided the formation of tremolite from olivine and diopside, Mg-hornblende and actinolite from diopside, Mg-chlorite from pleonaste, and the formation of compositional zoning in amphiboles with cores composed of Mg-hornblende to edenite and border of actinolite.

The dating of the alkali-feldspar granite resulted in the age of *ca.* 540 Ma, interpreted as the magmatic crystallization age and thus the approximate time of the skarn generation. According to this result and because of the absence of deformation in these rocks, the skarns related to the alkali-feldspar granite and the monzogranite are younger than those ones related to the metamafic dykes and must have been formed in the late- to post-collisional stage of the Araçuaí orogen.

CONCLUSIONS

Two different skarn types are found in the important marble quarries that belong to the Paraíba do Sul Complex in the region of Cachoeiro de Itapemirim, southern Araçuaí orogen: skarns related to granite dykes and skarns related to metamafic bodies. The skarns associated with undeformed and therefore late- to post-tectonic granite dykes are the largest, up to1.5 m wide. They are strongly zoned, showing distinct mineralogical bands due to the migration of silica and magnesia in response to the high chemical potential gradient between the dykes and their country rocks. Endoskarns are composed of *diopside + scapolite*, while exoskarns, by *diopside* and by *tremolite + carbonate*.

The primary origin of the metamafic rocks, if dykes or flows, could not be clearly depicted during fieldwork due to their intense deformation and metamorphism under granulite facies conditions. Their skarns are composed of poorly defined zones of *carbonate + olivine*, and of *diopside + hornblende*. It is probable that metamorphic overprinting erased part of the primary features and even the original mineralogy of the skarns.

Comparing the mineralogy of skarns of the two igneous rock types, it can be depicted that the presence of abundant scapolite is diagnostic for the granite skarns, while olivine is conspicuous for the mafic dykes.

The obtained concordant age of *ca.* 540 Ma is interpreted as the age of magmatic crystallization of the felsic dyke, which generated the largest skarn. This age corresponds to the late- to post-collisional stage of the Araçuaí orogen.

In case the metamafic rocks were flows, and therefore coeval with the deposition of the protolith of the marbles, they must be younger than the maximum depositional age of 619 Ma (Medeiros Junior 2016) and *ca.* 631 Ma (Noce *et al.* 2004) of the Paraíba do Sul sediments. If they were dykes, they must be younger than the carbonaceous rocks. However, in both cases the mafic rocks are older than the syn-collisional metamorphic event that affected the Aracuaí orogen dated between 580 and 560 Ma (Pedrosa-Soares & Wiedemann-Leonardos 2000, Pedrosa-Soares *et al.* 2001, 2007, 2011, Silva *et al.* 2005). Therefore, the age of the mafic rocks, either if dykes or flows, and their skarns, is constrained between the two mentioned ages.

ACKNOWLEDGEMENTS

The authors thank Research Support Foundation of the State of Minas Gerais (FAPEMIG) (CRA-APQ-02206-11) for financial support. R. B. Mesquita thanks National Counsel of Technological and Scientific Development (CNPq) for the MSc. scholarship, and gratefully acknowledges CPRM (Geological Survey of Brazil) for the comprehension about the MSc's activities. The authors are also grateful to the Microanalysis Laboratory of the Universidade Federal de Ouro Preto, a member of the Microscopy and Microanalysis Network of Minas Gerais State/Brazil/FAPEMIG.

REFERENCES

Almeida F.F.M. 1977. O Cráton do São Francisco. *Revista Brasileira de Geociências*, **7**:285-295.

Einaudi M.T., Meinert L.D., Newberry. 1981. Skarn deposits. *Economic Geology*, **75**:317-391.

Einaudi M.T., Burt D.M. 1982. Introduction – terminology, classification, and composition of skarn deposits. *Economic Geology*, **77**(4):745-754.

Jordt-Evangelista H., Viana D.J. 2000. Mármores da região de Itaoca (ES) e skarns no contato com diques máficos e félsicos: mineralogia e petrogênese. *Geonomos*, **8**(2):61-67.

Ludwig K.R. 2012. Isoplot/Ex Version 3.75: A Geochronological Toolkit for Microsoft Excel. *Berkeley Geochronology Center*, Berkeley, CA, Special Publication, **5**, 72p.

Medeiros Júnior E.B. 2016. Evolução petrogenética de terrenos granulíticos nos estados de Minas Gerais e Espírito Santo. Ouro Preto. Tese de Doutorado, Departamento de Geologia, Universidade Federal de Ouro Preto, 271p.

Meinert L.D. 1992. Skarns and skarn deposits. *Geoscience Canada*, **19**(4):145-162.

Mesquita R.B. 2016. Petrogênese, geoquímica, balanço de massa e idade de escarnitos associados a diques félsicos e máficos do Complexo Paraíba do Sul, sul do Espírito Santo. Ouro Preto. Dissertação de Mestrado, Departamento de Geologia, Universidade Federal de Ouro Preto, 123p.

Nasdala L., Hofmeister W., Norberg N., Mattinson J.M., Corfu F., Dörr W., Kamo S.L., Kennedy A.K., Kronz A., Reiners P.W., Frei D., Košler J., Wan Y., Götze J., Häger T., Kröner A., Valley J.W. 2008b. Zircon M257 – a homogeneous natural reference material for the ion microprobe U-Pb analysis of zircon. *Geostandard and Geoanalytical Reseach*, **32**:247-265.

Noce C.M., Pedrosa-Soares A.C., Piuzana D., Armstrong R., Laux J.H., Campos C.M., Medeiros S.R. 2004. Ages of sedimentation of the kinzigitic Complex and of a late orogenic termal episode in the Araçuaí orogen, northern Espírito Santo State, Brazil: zircon and monazite U-Pb SHRIMP and ID-TIMS data. *Revista Brasileira de Geociências*, **34**(4):587-592.

Oliveira J.P., Mendes R.S., Faria T.G., Fernandes V.M.T., Moura D.F.A., Fontana E.A., Santos G.A., Gomes I.R., Nascimento F.J.S., Barbosa K.V., Freitas L.G.B.G., Kumaira S., Torres L.F., Alves M.I., Gasparini S.P., Pereira V.V., Silva H.V., Medeiros J.D.C., Macedo R.S., Ribeiro T.B.V., Candotti C.S., Martins M.E., Davel R.F., Silva V.B., Guadagnin F., Campos R.S., Medeiros Júnior E.B. 2012. *Nota explicativa do Projeto Vargem Alta: Mapeamento Geológico 1:25.000 de parte das folhas Cachoeiro de Itapemirim SF.24-V-A-V-4 e Castelo SF.24-V-A-V-2.* Alegre, UFES, Departamento de Geologia, 55p.

Oliveira L.J.R. 2012. Petrogênese de skarns do Complexo Paraíba do Sul, Espírito Santo. Departamento de Geologia, Universidade Federal de Ouro Preto, Ouro Perto, Monografia, 52p.

Pedrosa-Soares A.C., Noce C.M., Vidal P., Monteiro R., Leonardos O.H. 1992. Toward a new tectonic model for the Late Proterzoic Araçuaí (SE Brazil) – West Congolian (SW Africa) Belt. *Journal of South American Earth Sciences*, **6**:33-47.

Pedrosa-Soares A.C. & Wiedemann-Leonardos C.M. 2000. Evolution of the Araçuaí Belt and its connection to the Ribeira Belt, Eastern Brazil. *In*: U. Cordani, E. Milani, A. Thomaz-Filho, D.A. Campos (Eds.) *Tectonic Evolution of South America*. São Paulo, Sociedade Brasileira de Geologia, p. 265-285.

Pedrosa-Soares A.C., Noce C.M., Wiedemann C.M., Pinto C.P. 2001. The Araçuaí–West Congo orogen in Brazil: An overview of a confined orogen formed during Gondwanland assembly. *Precambrian Research*, **110**:307-323.

Pedrosa-Soares A.C., Noce C.M, Alkmim F.F., Silva L.C., Babinski M., Cordani U., Castañeda C. 2007. Orógeno Araçuaí: síntese do conhecimento 30 anos após Almeida 1977. *Geonomos*, **15**(1):1-16.

Pedrosa-Soares A.C., Campos C.P., Noce C., Silva L.C., Novo T., Roncato J, Medeiros S., Castañeda C., Queiroga G., Dantas E., Dussin I., Alkmim F. 2011. Late Neoproterozoic-Cambrian granitic magmatism in the Araçuaí orogen (Brazil), the Eastern Brazilian Pegmatite Province and related mineral resources. *Geological Society, London, Special Publications*, **350**:25-51.

Porada H. 1989. Pan-African rifting and orogenesis in southern to equatorial Africa and Eastern Brazil. *Precambrian Research*, **44**:103-136.

Richard L.R. 1995. Mineralogical and petrological data processing system. Minpet for Windows, version 2.02. MinPet Geological Software, Canada.

Romano R., Lana C., Alkmim F.F., Stevens G., Armstrong R. 2013. Stabilization of the southern portion of the Sao Francisco craton, SE Brazil, through a long-lived period of potassic magmatism. *Precambrian Research*, **224**:143-159.

Silva L.C., McNaughton N.J., Armstrong R., Hartmann L., Fletcher I. 2005. The Neoproterozoic Mantiqueira Province and its African connections. *Precambrian Research*, **136**:203-240.

Takenaka L., Lana C., Scholz R., Nalini H., Tropia A. 2015 Optimization of the in-situ U-Pb age dating method via LA-Quadrupole-ICP-MS with applications to the timing of U-Zr-Mo mineralization in the Poços de Caldas Alkaline Complex, SE Brazil. *Journal of South American Earth Sciences*, **62**:70-79.

Tupinambá M., Heilbron M., Duarte B.P., Nogueira J.R., Valladares C., Almeida J., Silva L.G.E., Medeiros S.R., Almeida C.G., Miranda A., Ragatky C.D., Mendes J., Ludka I. 2007. Geologia da Faixa Ribeira Setentrional: estado da arte e conexões com a Faixa Araçuaí. *Geonomos*, **15**(1):67-79.

van Achterbergh E., Ryan C.G., Jackson S.E., Griffin W.L. 2001. Data reduction software for LA-ICP-MS: appendix. In: Canada, Association Canada (MAC), 239p. (Short Course Series 29).

Vieira V.S. 1997. *Programa de Levantamentos Geológicos Básicos do Brasil, Cachoeiro do Itapemirim, Folha SF.24-V-A. Escala 1:250.000.* Brasília, DNPM/CPRM, 99p.

Available at www.sbgeo.org.br